Clean Energy Market Connectedness and Investment Strategies: New Evidence from DCC-GARCH R^2 Decomposed Connectedness Measures

Teodoro Cocca[a], David Gabauer[a, *], and Stefan Pomberger[a]

[a] *Institute of Corporate Finance, Johannes Kepler University, Linz, Austria.*
[*] *Corresponding author: david.gabauer@hotmail.com.*

Abstract

In this study, we investigate the return propagation mechanism across four clean energy indices, namely, the NASDAQ OMX Green Economy Index, NASDAQ OMX Solar Energy Index, NASDAQ OMX Wind Energy Index, and NASDAQ OMX Geothermal Energy Index ranging from December 21st, 2010 until June 2nd, 2023 by using a novel DCC-GARCH-based R^2 decomposed connectedness approach. This framework allows us to efficiently decompose dynamic conditional R^2 goodness-of-fit measures into its decomposed components. Furthermore, we introduce the concept of minimum R^2 decomposed connectedness portfolios and multivariate hedging portfolios. We find that the dynamic total connectedness is heterogeneous over time and economic-event dependent. In addition, the empirical results highlight that the NASDAQ OMX Green Economy Index is a net transmitter of shocks while all others are net receivers of shocks. Finally, we find that our proposed portfolio technique outperforms the NASDAQ OMX Green Economy Index as well as all alternative multivariate portfolio techniques regarding the hedging effectiveness score and the Sharpe ratio.

Keywords: DCC-GARCH; dynamic connectedness; contemporaneous connectedness; dynamic conditional R^2; R^2 decomposition; multivariate hedging portfolios; multivariate minimum risk portfolios.
JEL codes: C50; F30; G15.

1 Introduction

The alarming escalation of climate change in recent times, along with its catastrophic consequences necessitates immediate action to minimize greenhouse gas emissions and prevent irreversible damage to the global ecosystem. Governments worldwide have emphasized the importance of promoting a gradual and well-structured transition to clean energy, with the goal of sustainable economic development. In alignment with the 2015 Paris Agreement, countries invest substantially in green energy to mitigate greenhouse gases. This shift towards green finance plays a crucial role in directing capital investments into environmentally friendly projects, which supports the development of a net-zero economy and offers significant environmental benefits (Alkathery et al., 2022; Zhang et al., 2023; Demiralay et al., 2023).

Recent evidence suggests that the clean energy sector is undergoing substantial growth not only in terms of a growing share of renewable energy in the production of electricity but also in terms of net investments in the clean energy sector per se (see, inter alia, Bloomberg, 2019; Dutta, 2019; Jaeger, 2021; International Energy Agency, 2022; Lee et al., 2023). It follows that the stock market for renewable energy has a key role to play, providing funds in support of the transition towards clean energy. In this regard, countries in pursuit of sustainable development goals and smaller fossil fuel consumption may be in a better position to achieve these objectives under the premise of a well-developed and financially solid stock market for clean energy (Zeqiraj et al., 2020; Lv et al., 2023).

Motivated by such dynamics and the potential impact of the stock market on government policies aiming to achieve crucial sustainability goals, in this paper we focus on the investigation of the financial stability of the renewable energy sector, considering that the performance and growth of clean energy indices may influence policy and investment decisions. In effect, our motivation relates to the potential negative impact on the process of achieving sustainable goals, stemming from volatility fluctuations of publically traded companies involved in the production of clean energy. It should be noted that, in order to capture these fluctuations different financial indices have been suggested (Burke and Stephens, 2018). One prominent set of clean energy indices is the NASDAQ OMX Green Economy Index Family. To the best of our knowledge, this is the

only set of indices that covers Solar, Wind, and Geothermal Energy Indices separately.

With these in mind, the objective of our study is to investigate network dynamics across clean energy stocks that may affect stability in the clean energy sector and, by implication, the overall transition towards sustainable development. By considering network dynamics within the clean energy sector, we attain a better understanding of the underlying transmission mechanisms that affect the potential growth of the different sources of clean energy and we underscore potential sources of systemic risk that threaten financial stability and sustainable growth in the clean energy market. To be more explicit, our main objective is to investigate the propagation mechanism between the NASDAQ OMX Green Economy Index and its subset of alternative energy indices – including the NASDAQ OMX Solar Energy Index, NASDAQ OMX Wind Energy Index, and NASDAQ OMX Geothermal Energy Index – by using the DCC-GARCH R2 decomposed connectedness approach and to create various bivariate and multivariate portfolios to decrease the investment risk and increase the reward-to-volatility ratio.

Hence, we position our study among the recent relevant literature that focuses on connectedness dynamics across networks of clean energy assets (see, inter alia, Chatziantoniou et al., 2022; Naeem et al., 2022; Demiralay et al., 2023). A more explicit look at the relevant literature is provided in the Literature Review Section.

In turn, the contribution of our study is threefold. First, we introduce the novel DCC-GARCH R^2 decomposed connectedness approach which allows us to examine conditional variance-covariances, correlations, R^2 goodness-of-fit measures, and decomposed R^2 contributions in a dynamic fashion. This does not only introduce a new type of connectedness approach, but it also expands on the DCC-GARCH toolbox by highlighting how the DCC-GARCH model can be demonstrated as a generalization of multiple linear regression models and how R^2 and decomposed R^2 contributions can be computed. Another crucial aspect of this approach is the concept of dynamic conditional R^2 goodness-of-fit measure, which helps determine the predictability of the left-hand side (LHS) at different points in time. A higher dynamic conditional R^2 measure indicates a greater likelihood of understanding how a specific series responds to a shock in another series. The larger the dynamic conditional R^2 measure, the more likely it is that we can

explain how a particular series will adjust to a shock in another series. By concentrating on this particular group of alternative energy indices, we aim to understand how key technologies, which currently attract over 75% of global investment in renewable energy (International Renewable Energy Agency, 2021), contribute to the overall clean energy transmission mechanism.

Second, we put forth two novel portfolio methodologies, namely the minimum bivariate R^2 portfolio and the minimum R^2 decomposed connectedness portfolio. These portfolios illustrate a substantial reduction in investment risk as well as increasing in reward-to-volatility ratio which is of crucial importance due to the unique technical characteristics of clean energy markets which make them more susceptible to speculative shocks compared to traditional energy markets (Bohl et al., 2013). The primary objective of these techniques is to minimize the interdependencies among financial assets. We proceed to juxtapose this framework against well-known benchmark portfolio techniques as well as the Green Economy Index. Furthermore, we elucidate the utilization of dynamic conditional beta coefficients for the construction of a multivariate hedging portfolio. The efficacy of all portfolios is assessed based on the hedging effectiveness proposed by Ederington (1979) and the Sharpe ratio introduced by (Sharpe, 1994).

Third, we provide new empirical evidence to the renewable energy literature which is rather silent when it comes to examining the market risk of the renewable energy sector and investigating the transmission mechanism of renewable energy components such as wind, solar, and geothermal energy.

Our findings highlight that the market risk is time-varying and economic-event dependent. Notably, we observe peaks in market risk during key events such as the Arab Spring in 2012, the COVID-19 pandemic in 2020, and the Russo-Ukrainian war in 2022. Additionally, our findings indicate that the Green Economy Index serves as a net transmitter of shocks, while all alternative energy indices act as net receivers of shocks throughout the analyzed period. Furthermore, our analysis demonstrates that all connectedness-based portfolio techniques surpass both the minimum variance and minimum correlation portfolios in terms of hedging effectiveness and Sharpe ratios.

The remainder of the paper is structured as follows. Section 2 provides an overview of

the state-of-the-art literature. Section 3 introduces and describes the employed dataset while Section 4 outlines our implemented methodologies. Section 5 interprets and discusses the obtained empirical results. Finally, Section 6 concludes the study.

2 Literature review

Recently, there has been significant attention focused on investigating the propagation mechanism of clean energy assets. Many researchers, including including Chatziantoniou et al. (2022), Naeem et al. (2022), Ha (2023), Demiralay et al. (2023), and Tiwari et al. (2022), have explored the interdependencies and spillovers among clean energy indices. Connectedness-dynamics lie at the heart of this study and therefore the relevant strand of the connectedness literature constitutes our main point of reference. In the pages that follow, we provide an essential account of relevant studies in order to accentuate the positioning of our study among existing literature and to better highlight our motivation.

2.1 Clean energy 'across asset' connectedness

A growing body of literature has emerged, examining the interconnectedness between the clean energy market and various other domains. Among the many, Ren and Lucey (2022), Li et al. (2023a), and Patel et al. (2023) have investigated the relationship between clean energy and cryptocurrencies, while Zeng et al. (2023) have explored its connection with agricultural commodities. Furthermore, Umar et al. (2022), Bouoiyour et al. (2023), Gong et al. (2023), and Li et al. (2023b) have studied the association between clean energy and traditional energy markets.

In turn, the impact of clean energy on equity markets has been analyzed by Kuang (2021), Broadstock et al. (2022), and Mensi et al. (2022). Finally, the interaction between clean energy and industrial/precious metal markets has been investigated by Gustafsson et al. (2022), Hanif et al. (2023), and Yahya et al. (2023).

In addition, Gong et al. (2023) utilize the quantile time-frequency connectedness approach introduced by Chatziantoniou et al. (2022) to examine the interconnections among Bio Fuel, Fuel Cell, Solar, Wind, and Geothermal energy indices, along with natural gas. The empirical findings suggest that natural gas plays a central role as the

primary transmitter of shocks, exerting a significant influence on the clean energy market. In other words, a shock in natural gas has a more substantial impact on clean energy indices compared to the reverse scenario. This discovery is further corroborated by Li et al. (2023a). Furthermore, the study reveals that crude oil acts as a net receiver in relation to all clean energy assets. By contrast, Zeng et al. (2023) apply the TVP-VAR connectedness approach (Antonakakis et al., 2020a) and obtain compelling evidence supporting the notion that Geothermal Energy and Bio/Clean Fuels have a significant influence on spillover shocks in grain commodity markets.

Along a similar vein, Li et al. (2023a) employ a quantile connectedness approach (Chatziantoniou et al., 2021) and show that the NASDAQ OMX Green Economy Index serves as the primary transmitter of shocks, both at the lower and upper ends of the quantile spectrum, affecting the Chinese stock market and Bitcoin. These findings align with the results obtained by Mensi et al. (2022), demonstrating the dominant impact of clean energy assets over the S&P500 across various quantiles.

2.2 Clean energy 'within-sector' connectedness

While the interdependencies across the clean energy market and other financial asset classes are well studied, our understanding of the internal relationships and spillover effects within the clean energy sector remains limited. In a recent study by Ha (2023), compelling evidence has emerged regarding the noteworthy association between solar energy, biogas energy, biofuel energy, geothermal energy, and carbon emission futures.

This relationship is particularly significant in both the low-frequency band spanning from 2020 to mid-2022 and the high-frequency band beginning in 2022 and extending to mid-2022, which coincides with the onset of the Russo-Ukrainian war. Furthermore, Dogan et al. (2022) conducted a comprehensive analysis of the transmission mechanism within the renewable energy sector. They specifically examined the S&P Green Bond Index, NASDAQ OMX BioFuels, NASDAQ OMX Fuel Cell, NASDAQ OMX Geothermal, NASDAQ OMX Solar, and NASDAQ OMX Wind Energy Index using TVP-VAR connectedness measures. The study spanned from August 1st, 2014 to February 4th, 2022. The findings indicate that the S&P Green Bond Index serves as the primary

recipient of shocks, influenced by all renewable energy assets. Notably, the empirical results highlight the presence of time-varying market risk, with the highest peak observed at the onset of the COVID-19 pandemic in early 2020.

In a separate investigation by Tiwari et al. (2022), the authors explored the propagation mechanism across various indices, including the S&P Green Bond, Solactive Global Solar, Solactive Global Wind, S&P Global Clean Energy, and Carbon Emissions. The study encompassed the period from January 4th, 2015 to September 22nd, 2020. Utilizing both LASSO-VAR and TVP-VAR-based connectedness measures, the authors found that the dynamic total connectedness varied over time, with two notable peaks occurring in 2016 and 2020. These peaks were associated with significant events such as the Chinese crisis, the OPEC cut, and the emergence of the COVID-19 pandemic.

Furthermore, a study conducted by Chatziantoniou et al. (2022) delved into the network dynamics of multiple clean energy indices, namely the S&P Global Clean Energy Index, S&P Green Bond Index, MSCI Global Environment, and Sustainability Index World. Spanning from November 28th, 2008 to January 12th, 2022, the researchers employed quantile time-frequency connectedness dynamics to examine the transmission of shocks within this network. The results highlighted the S&P Global Clean Energy Index as the primary transmitter of shocks, while the remaining indices were predominantly influenced by the network. Notably, the findings revealed that the MSCI Global Environment and Sustainability Index World acted as transmitters, while the S&P Global Clean Energy and S&P Green Bond Index served as recipients of short- and long-term frequency shocks in the transmission mechanism. Furthermore, it was observed that the degree of interconnectedness, both in terms of short-term and long-term frequency, increased at the lower and upper ends of the quantile spectrum. Additionally, Liu et al. (2021) conducted a study utilizing a time-varying copula and conditional Value-at-Risk model to explore the dependence and systemic risk between eight green bonds and clean energy assets. The findings strongly supported the presence of risk spillovers across these markets, reinforcing the interconnected nature of green bonds and clean energy assets.

2.3 Clean energy connectedness and investment portfolios

On another note, there is limited knowledge regarding the efficiency of bivariate and multivariate portfolios in the green bond and clean energy markets. While many studies have explored how clean energy assets can diversify other asset classes, little is known about the effectiveness of portfolios solely based on clean energy assets. For instance, Ren and Lucey (2022) provide suggestive evidence that clean energy can serve as a safe haven for dirty cryptocurrencies.

Similarly, Goodell et al. (2022) highlight that green assets support the diversification of Bitcoin. Asl et al. (2021) calculate bivariate optimal portfolio weights (Kroner and Ng, 1998) and bivariate hedge ratios (Kroner and Sultan, 1993) between natural gas and various clean energy assets. They find that the hedge ratio between S&P Global Clean Energy and natural gas is negative, while the hedge ratios with respect to Heating Oil, Gasoline, Crude Oil, and Propane are positive. This suggests that investors can hedge S&P Global Clean Energy by taking a long position in natural gas or short positions in other traditional energy assets. Interestingly, the optimal weight of S&P Global Clean Energy in bivariate portfolios consistently exceeds 50%, except when it comes to the S&P Global Oil Index.

In addition, Kuang (2021) shows that clean energy stocks outperform dirty stocks but underperform equity markets. Additionally, he observed significant variations in the risk-return profiles across clean energy sub-sectors and concluded that the minimum-tail risk strategy outperforms the minimum-variance portfolio (Markowitz, 1952).

Constructing portfolios that encompass various asset classes is often an attractive strategy for investors seeking to diversify their portfolio risk. However, it is crucial to emphasize the significance of building portfolios exclusively comprised of clean energy assets, as this approach not only contributes to improving the state of the environment and supporting green projects but also aligns with the objective of sustainable economic growth. In line with this objective, Tiwari et al. (2022) pursue a study involving the creation of bivariate hedge ratios, as well as bivariate and multivariate portfolios based on a selection of assets such as the S&P Green Bond, Solactive Global Solar, Solactive Global Wind, S&P Global Clean Energy, and Carbon Emissions. The findings of this

study highlight the inherent challenges in effectively hedging clean energy assets against each other, as evidenced by the limited effectiveness of hedging measures (Ederington, 1979).

However, it is worth noting that optimal bivariate portfolio weights have proven more successful in reducing portfolio variance, with the exception of the S&P Green Bond Index. Notably, neither the minimum variance portfolio nor the minimum correlation portfolio (Christoffersen et al., 2014) achieve significant risk reduction, whereas the minimum connectedness portfolio (Broadstock et al., 2022) successfully attain this objective.

Lastly, the study reveals that the minimum connectedness portfolio outperformed other portfolios during the COVID-19 pandemic period, highlighting its resilience and performance in challenging market conditions.

2.4 Clean energy connectedness and methods

While previous research has predominantly focused on investigating interdependencies using the connectedness approach (Diebold and Yılmaz, 2009, 2012, 2014), we align ourselves with this line of inquiry. However, the methodologies currently employed rely on rolling-window VAR or TVP-VAR models, which necessitate the standardization of spillovers through row sum normalization. This normalization technique has faced substantial criticism from Caloia et al. (2019), Lastrapes and Wiesen (2021), and Balcilar et al. (2021). To address this concern, we adopt the recently developed concept of R^2 decomposed connectedness measures (Balli et al., 2023; Naeem et al., 2023; Zhang et al., 2023).

Gabauer et al. (2023) have established a connection between R^2 measures and the generalized forecast error variance decompositions (GFEVD) concept proposed by Koop et al. (1996) and Pesaran and Shin (1998). Their work demonstrates that in the case of random walk series, the GFEVD collapses to bivariate R^2 goodness-of-fit measures.

Building upon this link, Naeem et al. (2023) suggest estimating multivariate linear regression (MLR) models and decomposing the R^2 goodness-of-fit measure, which always falls between zero and unity, using the R^2 decomposition method introduced by Genizi (1993). Balli et al. (2023) further extend this concept by incorporating lagged RHS

variables in the MLR, enabling the examination of both contemporaneous and lagged connectedness measures. Nonetheless, both frameworks rely on rolling-window techniques, which suffer from the multiple testing problem and may smooth out mean and volatility dynamics due to the window size chosen.

Consequently, the connectedness measures can be significantly affected by the arbitrarily selected window size. To address this limitation and provide truly time-varying connectedness measures, we employ the DCC-GARCH approach (Engle, 2002), which allows us to explore dynamic conditional correlations and covariances. Additionally, by leveraging these two measures, we can also present multivariate hedging portfolios that are based on the dynamic conditional betas (Engle, 2016) as well as two novel multivariate connectedness portfolios.

3 Data

This research study utilizes a daily dataset obtained from Datastream, which covers the period from December 1st, 2010 to June 2nd, 2023. The dataset focuses on four indices: NASDAQ OMX Green Economy Index (GRE), NASDAQ OMX Solar Energy Index (SOL), NASDAQ OMX Wind Energy Index (WIN), and NASDAQ OMX Geothermal Energy Index (GEO). The NASDAQ OMX Green Economy Index is a market-capitalization weighted benchmark crafted to monitor the performance of around 330 companies spanning various industries closely linked with sustainable development. Furthermore, the NASDAQ OMX Wind, Solar, and Geothermal Indices are sub-sector indices of the Green Economy Index designed to track companies that produce energy through wind, solar, and geothermal power, respectively.

Thus, the NASDAQ OMX Green Economy Index can be seen as a proxy for the clean energy market portfolio, as it comprises companies engaged in various subsectors associated with the green economy. These subsectors typically involve industries and technologies that prioritize environmental sustainability, renewable energy, clean technology, and other environmentally friendly practices. As a result, all the indices used in this study serve as indicators of the industry's progress, attracting attention from investors, policymakers, and stakeholders with an interest in sustainable development.

This study aims to examine the transmission mechanism among these indices, providing insights into the interdependencies and shock spillovers of assets. By monitoring, forecasting, and formulating economic policies accordingly, the aim is to prevent adverse spillovers that could lead to financial instability in the clean energy sector.

In order to adequately process the employed series, it is required that each series is stationary. Since the Elliott et al. (1996) unit-root test concludes that the raw series are non-stationary, we analyze the daily percentage changes of each series. Table 1 presents the summary statistics. Based on the standard two-sided t-test, the mean return of GRE, SOL, and WIN are positive and statistically significant at the 10% significance level. On average, SOL has the highest mean return, followed by WIN, GRE, and GEO. However, it's important to note that GEO's mean return does not demonstrate statistical significance at any conventional level. Notably, GRE has the lowest variance, while SOL exhibits the highest variance, making it the most volatile and risky asset. Additionally, the summary statistics indicate that GRE, SOL, and WIN are significantly left-skewed, whereas GEO is significantly right-skewed. This suggests a higher probability of extreme negative returns for GRE, SOL, and WIN, and the opposite for GEO. Moreover, all series are found to be significantly leptokurtic and non-normally distributed, indicating fatter tails compared to normally distributed series. Furthermore, all series are stationary and exhibit ARCH/GARCH errors, indicating mean-reverting processes with heteroscedastic volatilities. Finally, all Kendall rank correlation coefficients are positive and statistically significant, at least at the 1% significance level, implying that a positive change in one series results in a positive change in all other series.

[INSERT TABLE 1 AROUND HERE.]

4 Methodology

This section begins by exploring the core mechanics of the standard multivariate linear regression (MLR) model, aiming to establish the foundation for understanding how the DCC-GARCH model can be viewed as an extension of the MLR model. Following that, an overview of the DCC-GARCH model (Engle, 2002) will be presented, highlighting

the construction of dynamic conditional correlations and subsequently the dynamic conditional variance-covariances. The concept of dynamic conditional R^2 goodness-of-fit measure will then be introduced, along with its decomposition (Genizi, 1993) to provide detailed insights concerning the R^2 contribution of each RHS variable. Subsequently, the incorporation of the decomposed R^2 measures into the dynamic connectedness framework will be demonstrated and discussed in detail. Finally, both novel connectedness portfolios and the multivariate hedging portfolio are presented together with two benchmark portfolios and portfolio performance statistics.

4.1 Multivariate linear regression revisited

The MLR can be considered a workhorse in empirical finance and econometrics. In most studies, proposed models are compared to the MLR to illustrate the superiority of the outlined model. However, our case differs slightly as we illustrate the MLR as a fallback model of our employed DCC-GARCH model. In this context, we consider $\boldsymbol{Z} = [\boldsymbol{y}, \boldsymbol{X}]$ as a $T \times K+1$ dimensional matrix, encompassing both the dependent or LHS variable $\boldsymbol{y}$ and the independent or RHS variables $\boldsymbol{X}$ where K stands for the number of employed assets and T for the time period. For our purpose, we are interested in two fundamental concepts of the MLR, namely, the estimation of the regression coefficients and the computation of the R^2 goodness-of-fit measure. We start by outlining the MLR:

$$\boldsymbol{y} = \boldsymbol{X}\boldsymbol{b} + \boldsymbol{\epsilon} \tag{1}$$

where $\boldsymbol{\epsilon}$ and $\boldsymbol{b}$ represent an $T \times 1$ dimensional error vector and an $K \times 1$ dimension regression coefficient vector, respectively. To simplify matters, we make the assumption that all series, denoted as $\boldsymbol{Z}$, have been adjusted for the mean value, hence the exclusion of the intercept. To calculate the regression coefficients and determine the R^2 measure of goodness-of-fit, it is necessary to establish the partitioning of the variance-covariance and correlation matrices mentioned below.

$$\boldsymbol{H} = \left[\begin{array}{c|c} \boldsymbol{H}_{yy} & \boldsymbol{H}_{xy} \\ \hline \boldsymbol{H}_{yx} & \boldsymbol{H}_{xx} \end{array}\right], \quad \boldsymbol{R} = \left[\begin{array}{c|c} 1 & \boldsymbol{R}_{xy} \\ \hline \boldsymbol{R}_{yx} & \boldsymbol{R}_{xx} \end{array}\right].$$

$\boldsymbol{H}_{yy}$, $\boldsymbol{H}_{xx}$, and $\boldsymbol{H}_{xy}$ stand for the variance of the LHS variable, variance-covariances across the RHS variables, and the covariances between the RHS and LHS variables. The same concept applies to the correlation matrix, $\boldsymbol{R}$.

To obtain the regression coefficients, the following matrix operation must be performed:

$$\hat{\boldsymbol{b}} = (\boldsymbol{X}'\boldsymbol{X})^{-1}\boldsymbol{X}'\boldsymbol{y} \tag{2}$$

$$= \boldsymbol{H}_{xx}^{-1}\boldsymbol{H}_{xy}. \tag{3}$$

Consequently, the regression coefficients can be determined exclusively using the variance-covariance matrix, $\boldsymbol{H}$.

In order to compute the R^2 goodness-of-fit measure, we utilize an alternative concept by rearranging the following formula:

$$R^2 = 1 - \frac{(\boldsymbol{y} - \boldsymbol{X}\hat{\boldsymbol{b}})'(\boldsymbol{y} - \boldsymbol{X}\hat{\boldsymbol{b}})}{\boldsymbol{y}'\boldsymbol{y}} \tag{4}$$

$$= \boldsymbol{H}_{xy}'\boldsymbol{H}_{xx}^{-1}\boldsymbol{H}_{xy}\boldsymbol{H}_{yy}^{-1} \tag{5}$$

$$= \boldsymbol{R}_{xy}'\boldsymbol{R}_{xx}^{-1}\boldsymbol{R}_{xy}. \tag{6}$$

These relations illustrate that in order to calculate regression coefficients and the R^2 goodness-of-fit measure, one simply needs to have access to the unconditional variance-covariance matrix, $\boldsymbol{H}$. As the DCC-GARCH model provides us with dynamic conditional variance-covariances, we are able to compute dynamic conditional betas (Engle, 2016), along with dynamic conditional R^2 goodness-of-fit measures.

4.2 DCC-GARCH

In the spirit of Engle (2002), we can outline the dynamic conditional correlations generalized autoregressive conditional heteroscedasticity (DCC-GARCH) model as

follows[1]:

$$
\begin{aligned}
\boldsymbol{u}_t =& \boldsymbol{D}_t^{-1}\boldsymbol{z}_t \qquad \boldsymbol{z}_t \sim N(\boldsymbol{0}, \boldsymbol{H}_t), \quad \boldsymbol{u}_t \sim N(\boldsymbol{0}, \boldsymbol{I}), \quad \boldsymbol{D}_t = diag(\{h_{1t}^{1/2}, ..., h_{Kt}^{1/2}\}) \\
\boldsymbol{Q}_t =& (1-a-b)\bar{\boldsymbol{Q}} + a\boldsymbol{u}_{t-1}\boldsymbol{u}_{t-1}' + b\boldsymbol{Q}_{t-1} \\
\boldsymbol{R}_t =& diag(\boldsymbol{Q}_t)^{-1/2}\boldsymbol{Q}_t diag(\boldsymbol{Q}_t)^{-1/2} \\
\boldsymbol{H}_t =& \boldsymbol{D}_t\boldsymbol{R}_t\boldsymbol{D}_t
\end{aligned}
$$

where $\boldsymbol{z}_t$ and $\boldsymbol{u}_t$ are $K+1 \times 1$ dimensional return and standardized residual vectors, respectively. $\bar{\boldsymbol{Q}}_t$, $\boldsymbol{H}_t$, and $\boldsymbol{R}_t$ are $K+1 \times K+1$ dimensional unconditional variance, conditional variance-covariance, and conditional correlation matrix, respectively.

In a two-step estimation procedure, Engle (2002) demonstrated that estimating the DCC-GARCH model does not result in biased estimates. Initially, K univariate GARCH models are estimated to derive $\boldsymbol{D}_t$. Then, the shock parameter, a, and the persistence parameter, b, of the DCC-GARCH model are estimated to obtain $\boldsymbol{R}_t$ and subsequently $\boldsymbol{H}_t$. The log-likelihood function can be expressed as the combined sum of the volatility and correlation components:

$$L(\theta, \phi) = L_V(\theta) + L_C(\theta, \phi) \tag{7}$$

$$L_V(\theta) = -\frac{1}{2}\sum_{t=1}^{T}\sum_{i=1}^{K}(log(2\pi) + log(h_{i,t}) + \frac{z_{i,t}^2}{h_{i,t}}) \tag{8}$$

$$L_C(\theta, \phi) = -\frac{1}{2}\sum_{t=1}^{T}(Klog(2\pi) + 2log(|\boldsymbol{D}_t|) + log(|\boldsymbol{R}_t|) + \boldsymbol{u}_t'\boldsymbol{R}_t^{-1}\boldsymbol{u}_t) \tag{9}$$

where $L_V(\theta)$ and $L_C(\theta, \phi)$ stand for the volatility and correlation component of the log-likelihood function, respectively.

In the first step, the parameter θ represents the estimated univariate GARCH parameters, while the parameter ϕ represents the DCC-GARCH parameter in the second step. To maximize the log-likelihood, it is possible to maximize the first and second steps separately. Therefore, we maximize the log-likelihood based on Antonakakis et al. (2021)

[1]We have chosen the DCC-GARCH model because it is, aside from the CCC-GARCH model (Bollerslev, 1990), the only multivariate GARCH model that does not suffer from the curse of dimensionality. Additionally, it is the only multivariate GARCH model that allows conditional volatilities to follow different GARCH specifications.

selection criterion for univariate GARCH.[2] Antonakakis et al. (2021) utilize the omnibus family GARCH(1,1) model (see, Hansen and Lunde, 2005) proposed by (Hentschel, 1995):

$$h_t^{\lambda/2} = \omega + \alpha h_{t-1}^{\lambda/2}(|z_{t-1} - \eta| - \gamma(z_{t-1} - \zeta))^{\delta} + \beta h_{t-1}^{\lambda/2}. \tag{10}$$

This equation represents the Box-Cox transformation for the conditional standard deviation whose shape is determined by λ, and the parameter δ transforms the absolute value function which it subjects to rotations and shifts through the η and ζ parameters, respectively. Furthermore, ω, γ, α, and β represent the intercept, leverage term, shock, and persistence parameters, respectively. By restricting the parameters of the omnibus family GARCH model the following GARCH models can be estimated: GARCH (Bollerslev, 1986), Integrated GARCH (Engle and Bollerslev, 1986), Exponential GARCH (Nelson, 1991), Absolute Value GARCH (Schwert, 1990), Threshold GARCH (Zakoian, 1994), GJR-GARCH (Glosten et al., 1993), Nonlinear GARCH (Higgins et al., 1992), Nonlinear Asymmetric GARCH (Engle and Ng, 1993), and Asymmetric Power ARCH (Ding et al., 1993) models.[3]

To further enhance the maximization of the log-likelihood function, we adopt a method similar to Antonakakis et al. (2023) that introduces greater flexibility into the DCC-GARCH(1,1) model. This is achieved by estimating multiple bivariate DCC-GARCH models, allowing for varying parameters a and b. Estimating a single DCC-GARCH model for multiple assets assumes that the correlation dynamics between each pair are the same, resulting in identical parameter estimates for all pairs in the bivariate DCC-GARCH models. Moreover, this approach offers an additional benefit as it enables us to employ Engle and Sheppard (2001) DCC-GARCH test. This test allows us to estimate whether all pairs exhibit constant or dynamic conditional correlations, as well as dynamic conditional R2 goodness-of-fit measures.

[2]In simple terms, Antonakakis et al. (2021) introduce a univariate GARCH selection criterion, which is essentially an adjusted Bayesian Information Criterion (BIC). This criterion not only penalizes based on the total number of parameters but also considers the number of statistically insignificant parameters. Moreover, it incorporates knock-out criteria derived from significant misspecification test statistics such as VaR, CVaR, VaR Duration, Sign Bias, and Q2(20) test statistics. For more details, interested readers are directed to Antonakakis et al. (2021).

[3]For detailed information about the parameter restrictions as well as on conditional distributions, interested readers are referred to Ghalanos (2020).

If both variances remain constant over time (first stage) and all correlations are also constant (second stage), the estimated regression coefficients and R^2 will be identical to those retrieved from the MLR model. The statistical significance of first-stage regression coefficients can be verified by the magnitude of the t-test while the DCC-GARCH test of Engle and Sheppard (2001) is used to test whether we deal with constant conditional correlations (Bollerslev, 1990) or dynamic conditional correlations (Engle, 2002). Therefore, the DCC-GARCH model can be seen as an extension of the MLR model.

4.3 Dynamic conditional R^2 and R^2 decomposed measures

In order to compute the dynamic conditional R^2 goodness-of-fit measure, we simply replace the components of $\boldsymbol{H}$ in Equation (6) by the dynamic components of $\boldsymbol{H}_t$. Thus, dynamic conditional R^2 goodness-of-fit measures are obtained as follows,

$$R_t^2 = \boldsymbol{R}'_{xy,t}\boldsymbol{R}_{xx,t}^{-1}\boldsymbol{R}_{xy,t}. \tag{11}$$

Dynamic conditional R^2 goodness-of-fit measures are of crucial interest as they provide an assessment of the predictive power or explanatory ability of a statistical model in a time-varying fashion. If a series is hedged with another, the use of high dynamic conditional R^2 measures will indicate the potential success of the hedging strategy, as it demonstrates that the variability of the series can be significantly explained by a single variable. Furthermore, in terms of stock selection and risk management, high dynamic conditional R^2 values are highly relevant given that they provide information about expected future dependencies.

As pointed out in Gabauer et al. (2023), the sum of bivariate R^2 measures is unlikely to be equal to the R^2 measure of an MLR since chances are high that the RHS variables are correlated with each other. This is exactly the problem Genizi (1993) dealt with when developing his R^2 decomposition procedure. Fortunately, this procedure can be reformulated in order that it solely depends on the correlation matrix. The initial idea has been that K correlated series are transformed into K independent latent series, $\boldsymbol{f}_t$, by means of principal component analysis (PCA) in order to preserve 100% of the variation of

the k correlated series. By assuming that the correlated series have a mean of zero and unit variance, the variance-covariance matrix is equal to the correlation matrix. This is true as the correlation matrix is nothing else than a standardized variance-covariance matrix. Thus, in order to make the RHS variables independent of each other the symmetric and positive definite $\boldsymbol{R}_{xx,t}$ matrix will be decomposed using the eigenvalue decomposition. The following set of equations will describe how the R^2 decomposition procedure is conducted:

$$\boldsymbol{R}_{xx,t} = \boldsymbol{V}_t \boldsymbol{\Lambda}_t^2 \boldsymbol{V}_t = \boldsymbol{R}_{xf,t} \boldsymbol{R}'_{xf,t} \tag{12}$$

$$\boldsymbol{R}_{xf,t} = \boldsymbol{V}_t \boldsymbol{\Lambda}_t \boldsymbol{V}'_t \tag{13}$$

$$\boldsymbol{R}_t^2 = \boldsymbol{R}_{xf,t}^2 (\boldsymbol{R}_{xf,t}^{-1} \boldsymbol{R}_{xy,t})^2 \tag{14}$$

$$= \boldsymbol{R}_{xf,t}^2 \boldsymbol{R}_{fy,t}^2 \tag{15}$$

where $\boldsymbol{V}_t$ represents the eigenvectors and $\boldsymbol{\Lambda}_t^2$ the diagonal eigenvalue matrix obtained by decomposing $\boldsymbol{R}_{xx,t}$. The square root of the $\boldsymbol{R}_{xx,t}$ is then equal to the correlations between $\boldsymbol{x}_t$ and $\boldsymbol{f}_t$, $\boldsymbol{R}_{xf,t}$. Finally, the $K \times 1$ decomposed R^2 vector, $\boldsymbol{R}_t^2$ is obtained by the matrix product of $\boldsymbol{R}_{xf,t}^2$ and $\boldsymbol{R}_{fy,t}^2$. From an intuitive standpoint, if we consider the squared sum of the correlations between the LHS variable, $\boldsymbol{y}_t$, and the latent variables, we can observe that it is equivalent to R^2. This is because it represents the special scenario where the sum of bivariate R^2 measures matches the R^2 value obtained from an MLR where the LHS variable is regressed on all latent variables. It is important to highlight that in bivariate regression models, R^2 is equal to the squared correlation between the LHS and RHS variables. Since $\boldsymbol{R}_{xf,t}^2$ possesses the property of having row sums and column sums equal to one, it quantifies the impact of RHS variables in predicting the LHS variable.

4.4 Dynamic connectedness measures

By investigating the propagation mechanism of financial markets, we are able to provide relevant insights on several crucial economic aspects. Firstly, the analysis sheds light on the current market risk, allowing for a comprehensive understanding of the prevailing market conditions. Secondly, it assesses the prediction accuracy of the network, enabling more reliable predictions as well as revealing essential spillover channels. Furthermore, we identify whether variables act as net transmitters or net receivers of shocks, providing

a deeper understanding of financial market contagion.

In accordance with the connectedness approach of Diebold and Yılmaz (2012, 2014), we introduce a novel framework where the conventional scaled GFEVD matrix is replaced by the R^2 decomposition matrix, $\boldsymbol{R}^{2d}$. This matrix is retrieved by changing K times the LHS and RHS variables and stacking the R^2 decomposed measures in an iterative manner. Thus, $\boldsymbol{R}^{2d}_t = [\boldsymbol{R}^2_{1,t}, ..., \boldsymbol{R}^2_{i,t}, ..., \boldsymbol{R}^2_{K,t}]$. Table 2 represents the revised schematic of the DCC-GARCH R^2 decomposed connectedness approach in time t:

[INSERT TABLE 2 AROUND HERE.]

The unity values on the diagonal of the connectedness tables can be viewed in a similar manner to the unity values on the diagonal of a correlation matrix. Meanwhile, the off-diagonal elements represent the predictive contribution series j has on series i. Consequently, $R^{2d}_{12,t}$ stands for the predictive contribution of series 2 on series 1 in time t. By summing up the predictive contribution all series j have on series i in time t, we obtain the *total directional connectedness FROM others* which is equal to the R^2 goodness-of-fit measure where series i is considered as the LHS variable while the others are RHS variables:

$$FROM_{i,t} = \sum_{k=1,k\neq i}^{K} \boldsymbol{R}^{2d}_{ik,t} = R^2_{i,t}. \tag{16}$$

On the contrary, by aggregating the predictive contribution series i has on all other variables j in time t, we retrieve the *total directional connectedness TO others* demonstrating the overall predictive relevance variable i holds for the network:

$$TO_{i,t} = \sum_{k=1,k\neq i}^{K} \boldsymbol{R}^{2d}_{ki,t}. \tag{17}$$

The difference between the *total directional connectedness TO* and *FROM others* is defined as the *NET total connectedness* which reports the importance of variable i concerning its predictive performance:

$$NET_{i,t} = TO_{i,t} - FROM_{i,t}. \tag{18}$$

If $NET_{i,t} > 0$ ($NET_{i,t} < 0$), variable i is considered as a net transmitter (receiver) of shocks in time t. The rationale behind being a net transmitter of shock is that whenever a shock in variable i occurs it is assumed that all other variables j will be adjusted to this shock due to the contemporaneous relation and its predictive contribution.

Furthermore, the *net pairwise directional connectedness* illustrates the net transmission on the bilateral level. The $NPDC_{ij,t}$ represents the difference in the predictive contribution between variable i and variable j in time t:

$$NPDC_{ij,t} = \boldsymbol{R}^{2d}_{ij,t} - \boldsymbol{R}^{2d}_{ji,t}. \tag{19}$$

Whenever variable i contributes more (less) to the prediction of variable j than vice versa in time t, $NPDC_{ij,t} > 0$ ($NPDC_{ij,t} < 0$).

We now turn to the cornerstone of the connectedness approach, the total connectedness index (TCI) which assesses the interdependence within the network and is often used as a proxy for market risk. As the TCI is considered to be equal to the average *total directional connectedness TO others* or *total directional connectedness FROM others*, the TCI becomes equivalent to the averaged conditional R^2 goodness-of-fit measure:

$$TCI_t = \frac{1}{K}\sum_{k=1}^{K} TO_{k,t} = \frac{1}{K}\sum_{k=1}^{K} FROM_{k,t} == \frac{1}{K}\sum_{k=1}^{K} R^2_{k,t}. \tag{20}$$

Since R^2 falls between zero and one, the Total Connectedness Index (TCI) also falls within this range, effectively solving the problem of normalizing connectedness (see, Caloia et al., 2019; Lastrapes and Wiesen, 2021; Chatziantoniou and Gabauer, 2021; Balcilar et al., 2021). The intuition behind this is that the TCI tends to be high when series are highly correlated and moving in the same direction. This is particularly evident during periods of financial turbulence when a majority of financial assets experience significant negative percentage changes.

Finally, we introduce two pairwise connectedness index (PCI) approaches, which operate similarly to the TCI but focus on bilateral connections. The original PCI metric

has been proposed by Chatziantoniou and Gabauer (2021) and can be computed as follows,

$$PCI^{C}_{ij,t} = 2 \cdot \left(\frac{\boldsymbol{R}^{2,d}_{ij} + \boldsymbol{R}^{2,d}_{ji}}{\boldsymbol{R}^{2,d}_{ii} + \boldsymbol{R}^{2,d}_{ij} + \boldsymbol{R}^{2,d}_{ij} + \boldsymbol{R}^{2,d}_{jj}} \right) \tag{21}$$

while the second PCI approach is based upon the model-free connectedness approach of Gabauer et al. (2023). Interestingly, this metric is solely based on the dynamic conditional correlations of the DCC-GARCH model:

$$PCI^{R}_{ij,t} = \frac{2 \cdot \boldsymbol{R}^{2}_{ij,t}}{1 + \boldsymbol{R}^{2}_{ij,t}} \tag{22}$$

Both PCI metrics are used to minimize the interdependencies in different portfolio strategies.

4.5 Multivariate portfolio analysis

This section aims to explore various portfolio strategies, emphasizing the significance of adapting to evolving market conditions and the relevance of portfolio restructuring. It will delve into both bivariate and multivariate portfolio techniques, demonstrating the advantages of diversification and asset allocation in a dynamic environment. Initially, we will outline bivariate and multivariate hedging portfolios, followed by portfolios that prioritize mitigating investment risk. The evaluation of different portfolio strategies will be conducted using metrics such as the Sharpe ratio and hedging effectiveness.

4.5.1 Hedge ratios

We will begin by implementing the bivariate hedge strategy proposed by Kroner and Sultan (1993). Their study demonstrates the effectiveness of hedging the risk associated with holding a long position in asset i through an investment in a short position of asset j. In this context, the hedge ratio determines the expenses associated with hedging a 1 USD long position in asset i with a $HR_{ij,t}$ USD short position in asset j. This can be mathematically formulated as follows

$$HR_{ij,t} = \frac{\boldsymbol{H}_{ij,t}}{\boldsymbol{H}_{jj,t}} \tag{23}$$

where $\boldsymbol{H}_{ij,t}$ and $\boldsymbol{H}_{jj,t}$ stand for the conditional covariance between asset i and j and the conditional variance of asset j.

4.5.2 Multivariate hedging portfolio

The concept of the multivariate hedging strategy is derived from the dynamic conditional beta concept outlined in Engle (2016). In this strategy, the dynamic conditional beta indicates the investment amount in multiple short positions that act as a hedge for a 1 USD long position in $\boldsymbol{y}_t$. By employing this approach, we anticipate a larger reduction in portfolio risk and less volatile hedge ratios, which ultimately improves the predictability of future hedge ratios within the context of portfolio rebalancing strategies. The calculation of dynamic conditional betas is done in the following manner:

$$\boldsymbol{b}_t = \boldsymbol{H}_{xx,t}^{-1}\boldsymbol{H}_{xy,t}. \tag{24}$$

As a result, to hedge a 1 USD $\boldsymbol{y}_t$ position, one can invest $\boldsymbol{b}_t$ USD in shorting other assets. The performance of this strategy is expected to yield better results during periods where strong positive or negative correlations among assets are present, as well as when the level of predictive accuracy is high. Therefore, the dynamic conditional R^2 measures should be monitored when pursuing this strategy.

4.5.3 Optimal bivariate portfolio weights

To mitigate the risk of a two-asset portfolio in the face of volatile financial market movements, we utilize the optimal bivariate portfolio weight strategy proposed by Kroner and Ng (1998). This approach assumes that investors hold a portfolio with a no-shorting constraint. Furthermore, this approach assumes that expected returns are zero, and thereby the problem is to find the optimal portfolio weights that minimize the portfolio risk. We compute the portfolio weights of asset i using the following formula:

$$w_{ij,t} = \frac{\boldsymbol{H}_{jj,t} - \boldsymbol{H}_{ij,t}}{\boldsymbol{H}_{ii,t} - 2\boldsymbol{H}_{ij,t} + \boldsymbol{H}_{jj,t}}. \tag{25}$$

To ensure adherence to the no-shorting constraint - portfolio weights must fall between

zero and unit - the following restrictions are imposed on the weights:

$$w_{ij,t} = \begin{cases} 0 & \text{if } w_{ij,t} < 0 \\ w_{ij,t} & \text{if } 0 \leq w_{ji,t} \leq 1 \\ 1 & \text{if } w_{ij,t} > 1 \end{cases} \tag{26}$$

where $w_{ij,t}$ and $1 - w_{ij,t}$ are the weights of asset i and j in a 1 USD portfolio at time t.

4.5.4 Global minimum risk portfolios

In the pursuit of minimizing portfolio risk, we shift our focus towards multivariate portfolio strategies. These strategies, as explored by Markowitz (1952), Christoffersen et al. (2014), and Broadstock et al. (2022), are built on a common concept but employ distinct metrics for risk minimization. To provide a comprehensive understanding, we begin by outlining the general framework and subsequently delve into the process of obtaining diverse portfolio weights. The global minimum risk portfolio can be seen as a minimization optimization problem which can be formulated as follows,

$$\underset{\boldsymbol{w}_t}{\text{argmin}} \quad \boldsymbol{w}_t' \boldsymbol{P}_t \boldsymbol{w}_t \qquad \text{s.t.} \quad \boldsymbol{w}_t' \mathbf{1} = 1, \qquad \mathbf{0} \leq \boldsymbol{w}_t \leq \mathbf{1}. \tag{27}$$

where $\boldsymbol{w}$ denotes the $K \times 1$ dimensional portfolio weights vector in time t that results from minimizing the $K \times K$ dimensional asset risk matrix, $\boldsymbol{P}$. The portfolio risk minimization strategies have evolved over time. Initially, Markowitz (1952) proposed the use of the variance-covariance matrix, $\boldsymbol{H}_t$. However, Christoffersen et al. (2014) argued that minimizing the correlations, $\boldsymbol{R}_t$, is more relevant for risk reduction. Building on these studies, Broadstock et al. (2022) have demonstrated that minimizing $\boldsymbol{PCI}_t^C$ not only significantly reduces portfolio risk but also outperforms both the Markovitz and Christoffersen strategies. Inspired by the findings of Broadstock et al. (2022), we suggest adopting the approach of minimizing $\boldsymbol{PCI}_t^R$, which relies on dynamic conditional correlations. Additionally, we propose reducing interdependencies across assets by minimizing $\boldsymbol{R}_t^{2d}$.

4.5.5 Portfolio performance

The portfolio performance is assessed using two metrics: the Sharpe ratio (Sharpe, 1994) and the hedging effectiveness (Ederington, 1979).

The Sharpe ratio (SR), often referred to as the reward-to-volatility ratio, is calculated as follows,

$$SR = \frac{\bar{\boldsymbol{x}}_p}{\sqrt{var(\boldsymbol{x}_p)}} \tag{28}$$

where $\bar{\boldsymbol{x}}_p$ and $var(\boldsymbol{x}_p)$ stand for the average portfolio return and the portfolio variance, respectively. A higher SR indicates greater returns relative to the portfolio risk. By comparing the SR of different portfolios, we can determine the highest portfolio return given the same level of volatility. Alternatively, we use the Value-at-Risk and the conditional Value-at-Risk as the denominator.

Ederington (1979) introduced the concept of Hedging Effectiveness (HE) which provides insight into the degree of risk reduction achieved by investing in a portfolio rather than investing solely in a single asset i. To determine the significance of this reduction, we utilize the HE test statistics developed by Antonakakis et al. (2020b). The HE can be computed in the following manner,

$$HE_i = 1 - \frac{var(\boldsymbol{x}_p)}{var(\boldsymbol{x}_i)} \tag{29}$$

where $var(\boldsymbol{x}_i)$ denotes the variance of asset i, and HE_i provides information on the percentage-wise risk reduction by investing in a portfolio compared to asset i. Thus, A high (low) HE index indicates a high (low) risk reduction.

5 Empirical results

The empirical results section is organized as follows. We begin by presenting the DCC-GARCH estimation results and the selection of univariate GARCH models, including their misspecification tests. Moreover, we discuss and present the dynamic conditional R^2 and R^2 decomposed measures. Next, we proceed to discuss the outcomes of our proposed connectedness approach. Initially, we provide an overview of the clean

energy propagation dynamics through the use of averaged connectedness measures. Subsequently, we delve into the dynamic connectedness plots, offering a more detailed explanation. Finally, we concentrate on comparing bivariate and multivariate portfolio techniques and evaluate the performance of multivariate portfolios using various portfolio statistics.

5.1 DCC-GARCH estimation

Table 3 presents the estimation results of the bivariate mixed DCC-GARCH model. Following Antonakakis et al. (2021), we employ different models to capture the conditional volatility of GRE, SOL, WIN, and GEO, namely the exponential GARCH (Nelson, 1991), standard GARCH (Bollerslev, 1986), and twice the Threshold GARCH (Zakoian, 1994) models. Since the standardized residuals appear to be non-normally distributed, we enhance the modeling by incorporating Student's t, skew Student's t, and skew generalized error distributions, as recommended by the GARCH selection algorithm. Our findings indicate that, except for SOL, all models account for asymmetric effects, wherein negative returns increase conditional volatilities. It should be noted that the Exponential GARCH model effectively incorporates the scaled disturbance term to account for asymmetric effects. In contrast, the Threshold GARCH model utilizes an indicator variable to capture negative disturbances, elucidating the reason behind the negative sign of the leverage parameter in the former and the positive sign in the latter. Given the significance of all α and β coefficients, at least at the 10% level, we can conclude that variances exhibit time-varying behavior.

Furthermore, we observe a high degree of persistence in the conditional volatility, as shown by the proximity of all β coefficients to unity. Additionally, it is important to note that the data exhibit fat tails and skewed distributions, as reflected in the parameters of the conditional distribution. While the Student's t distribution approximates a normal distribution when the degree of freedom is 30, and the generalized error distribution approximates a normal distribution when the shape parameter is 2, it is evident that in all four cases, the standardized residuals display fat tails. Moreover, the statistically significant skewness parameters of GRE, SOL, and GEO indicate that the standardized

residual distributions are asymmetrical.

[INSERT TABLE 3 AROUND HERE.]

In addition, it is worth noting that all bivariate DCC-GARCH models identify the conditional correlations to be time-varying according to the DCC-GARCH test of Engle and Sheppard (2001). This is further supported by the statistical analysis presented in Table 3, which reveals that all multivariate DCC-GARCH parameters (a and b) are significantly different from zero at least at the 1% significance level. Estimated a parameters are located on the lower triangular, while the b parameters are reported on the upper triangular. In a similar fashion, we present the dynamic conditional correlations (lower triangular) and the degrees of freedom based on the Student's t distribution (upper triangular) for each bivariate DCC-GARCH model. Our findings demonstrate that all dynamic conditional correlations as well as the degrees of freedom are statistically significantly different at least at the 1% significance level.

To evaluate the presented GARCH specification, we performed different misspecification tests which are summarized in Table 4. A significant outcome in the Sign Bias test (Engle and Ng, 1993) would suggest incorporating (further) leverage parameters to account for asymmetric effects. The $Q^2(20)$ statistics (Fisher and Gallagher, 2012) were employed to determine whether additional α and β parameters are necessary to accurately capture conditional volatility. Non-significant test results indicate that the employed model effectively captures the conditional volatility.

[INSERT TABLE 4 AROUND HERE.]

We also utilized the Value-at-Risk (VaR) test proposed by Christoffersen (1998) to assess whether there is a statistically significant difference between observed losses and estimated VaR. Additionally, the conditional Value-at-Risk (CVaR) test by Christoffersen et al. (2001) is employed to evaluate the GARCH model's ability to estimate potential losses at the 5% quantile level. Finally, we apply the Value-at-Risk Duration (VaR Dur.) test by Christoffersen and Pelletier (2004) to examine the model's capability to capture the duration of extreme events. If the VaR Duration test is significant, it would imply that the model fails to accurately estimate the time duration of losses surpassing the VaR threshold.

The significance of any of these tests would suggest the consideration of an alternative GARCH model. Thus, the fact that none of the misspecification tests is significant at any conventional levels, we can conclude that the presented univariate GARCH models accurately capture conditional volatility and different VaR-based measures.

5.1.1 Dynamic conditional variance-covariances

Based upon the presented mixed bivariate DCC-GARCH estimation, we obtain dynamic conditional variance-covariances and dynamic conditional correlation measures.

Figure 1 presents the dynamic conditional variance-covariances. We find that SOL, WIN, and GEO are more volatile than GRE. Besides the individual volatility dynamics, we observe that three major volatility peaks can be observed in all series, namely, during the Arab Spring of 2012, the COVID-19 outbreak in 2020, and during the Russo-Ukrainian war in 2022. These three common volatility peaks are also shown in the conditional covariances which reflect bivariate interdependencies.

[INSERT FIGURE 1 AROUND HERE.]

5.1.2 Dynamic conditional betas

As previously demonstrated, the dynamic conditional betas can be computed based on the dynamic conditional variance-covariances. As shown in Figure 2 the interdependences between the employed series vary considerably. Notably, the pronounced variation in these interdependencies is primarily driven by the variances of SOL, WIN, and GEO, which are at least twice the size of GRE, as shown in Table 1. For comparison, we have included the regression coefficients of the associated OLS models. Noteworthy deviations from the OLS estimates are observed not only during periods of economic and financial turmoil but also amidst changes in the clean energy market. Interestingly, while all OLS estimates are significantly positive, we have observed some periods where dynamic conditional betas become negative, providing accurate updates on concealed market dynamics that cannot be captured by assuming a constant relationship throughout the sample period.

[INSERT FIGURE 2 AROUND HERE.]

5.1.3 Dynamic conditional correlations

Figure 3 illustrates the dynamic conditional correlations. A strong correlation between the GRE and SOL is evident, which can be attributed to the greater accessibility and versatility of solar energy compared to wind energy. This has led to a higher prevalence of solar energy installations, particularly in the last two decades, as the cost of such installations significantly decreased, resulting in substantial investments (Li et al., 2015). However, an interesting finding is a significant decline in this correlation between 2021 and mid-2022, which can potentially be linked to the supply chain disruptions caused by the COVID-19 pandemic.

[INSERT FIGURE 3 AROUND HERE.]

It is worth noting that the differences in correlation dynamics between the GRE and the three alternative energy sources are due to the utilization of bivariate DCC-GARCH models. If a single DCC-GARCH model were used, the evolution of dynamic conditional correlation would exhibit similar patterns, albeit with different magnitudes. Among the energy sources, GRE, SOL, and GEO display more volatile dynamic conditional correlations, whereas WIN demonstrates relatively stable relationships with the others.

An intriguing observation is that the dynamic conditional correlations involving GRE and the market portfolio consistently increase during times of economic and financial turmoil. However, an exception to this trend is seen in the relationship between GRE and GEO during the Russo-Ukrainian war. Lastly, it is important to note that all correlations remain strictly positive throughout the sample period, except for SOL and GEO, which exhibited short periods of slightly negative correlations during 2018 and at the end of the sample period.

5.1.4 Dynamic conditional R^2 and R^2 decomposed measures

In the following analysis, we examine the R^2 and decomposed R^2 goodness-of-fit measures computed using dynamic conditional correlations. Among the variables, GRE and SOL exhibit the highest R^2 values, explaining approximately 80% of the variation in the LHS variable. Overall, our findings suggest that GRE has the greatest explanatory power for alternative energy sources, followed by SOL, WIN, and GEO.

[INSERT FIGURE 4 AROUND HERE.]

Specifically, in the case of GRE, SOL accounts for the majority of the dynamics, followed by WIN, while GEO explains the smallest fraction. However, during the Arab Spring of 2012, SOL emerged as a more influential factor in explaining the variance in WIN compared to GRE or GEO. Nevertheless, over time, the predictive power of GRE increases, overshadowing SOL, and leaving only a small fraction of predictability for GEO. Interestingly, certain time periods reveal that SOL has a greater impact on the R^2 value of GEO. Conversely, WIN appears to have lesser significance in influencing the dynamics of GEO.

Notably, we observe that crisis periods are associated with increased R^2 goodness-of-fit measures, possibly due to high uncertainty leading to similar behaviors among series within the same sector. Consequently, high R^2 measures could be considered as a measure of market risk, indicating periods of heightened co-movements.

5.2 R^2 decomposed connectedness approach

We begin by explaining the averaged connectedness measures and then continue with the dynamic connectedness plots which provide us with a more detailed look at the time-varying behavior considering that averaged values are concealing dynamics.

The connectedness table is shown in Figure 5. As in the case of the correlation matrix, the diagonal is equal to 100% illustrating that regression of the series on itself would explain 100% of the variation in the LHS variable. The off-diagonal values illustrate the R^2 decomposed connectedness measures and thus the influence series j (column) has on series i (row). The row sum is equal to the R^2 goodness-of-fit measure of a time-varying multivariate linear regression model and represents the degree of variance explainability or predictability of the LHS variable by means of the RHS variables. Thus, R^2 is equal to the FROM total directional connectedness.

[INSERT TABLE 5 AROUND HERE.]

Furthermore, the TCI is equal to the average explained variance in the LHS variable. If the TCI is high it is assumed that the market risk is high due to the fact that all variables

are highly interconnected and thus illustrate a high level of co-movement. Finally, the TO total directional connectedness measure is equal to the sum of decomposed R^2 values of series i. Thus, it can be interpreted as the overall contribution of predictability series i has on all others in the network.

We find that the TCI is equal to 38.18% which means that the series in the network explain on average almost 40% of the variation in each variable. This can already be considered a high value given that we are dealing with a small network and that the degree of predictability strongly varies among assets. By having a closer look we see that GRE reaches an average FROM value of 54.93% which means that on average all other series explain 54.93% of the variation in GRE. SOL reaches a value of 46.42% while the FROM measure of WIN and GEO are equal to 29.92% and 21.45%, respectively. On the contrary, we find that GRE explains 60.05% of the variation while SOL, WIN, and GEO can determine 45.06%, 27.79%, and 19.81% of the variance in the network. Thus, GRE is considered the main net transmitter of shocks while SOL, WIN, and GEO are net receivers of shocks. On the net pairwise transmitting level, we see that GRE explains more of the variance of all others than others explain GRE variance. The second strongest predictive variable is SOL as it is on the net predicting end of WIN and GEO while WIN and GEO are mainly on the net receiving end of predictability.

5.2.1 Dynamic total connectedness

Figure 5 presents the dynamic total connectedness which illustrates the market risk in a time-varying fashion. As discussed in previous sections, we have compelling empirical evidence showing that significant events such as the Arab Spring in 2012, the COVID-19 pandemic outbreak in 2020, and the Russo-Ukrainian war in 2022 have had a profound impact on the clean energy market dynamics. The TCI supports these findings, with noticeable spikes observed in 2012, 2020, and 2022.

[INSERT FIGURE 5 AROUND HERE.]

Although the 2022 peak is relatively smaller compared to some peaks between 2013 and 2020, it's important to note that we reached an all-time low by the end of 2021. This suggests that the clean energy market is becoming more stable and less

susceptible to shocks from external markets, likely due to substantial investments and the implementation of Environmental, Social, and Governance (ESG) scores (see, Broadstock et al., 2021). Therefore, the 2022 peak holds significance as it experienced a rapid increase, doubling its previous level during the Russo-Ukrainian war. Importantly, these three peaks directly correlate with economic and financial crises, distinguishing them from other peaks. While the impacts of investments in solar, wind, and geothermal energy sectors are challenging to disentangle from one another, the TCI consistently demonstrates substantial differences associated with changing market conditions (see, Baruník and Křehlík, 2018; Bouri et al., 2021).

5.2.2 Net total directional connectedness

Finally, we focus on the net total directional connectedness which points out the series that are dominating the market or are dominated by the market. Figure 6 demonstrates that almost throughout the entire sample period GRE has been a net transmitter of shocks while WIN, SOL, and GEO are considered as net receivers of shocks. Interestingly, we find that WIN and SOL appear to be net transmitters during the Arab Spring of 2012 while GRE became a net receiver of shocks during this period. This could be partially attributed to the fact that the Arab Spring had a positive influence on the Desertec Industrial Initiative project (USD 550 billion) as awareness and interest in turning sunshine into energy has increased across North African and Middle Eastern economies (Kirschbaum, 2011).

[INSERT FIGURE 6 AROUND HERE.]

Another relevant observation is that SOL is on the net transmitting end at the sample period which might be another indication of how economic and financial crises shape the dynamics in the clean energy market. This is also in line with the finding that GRE almost became a net receiver at the beginning of the Russo-Ukrainian war and is at low levels at the end of the sample period. Also, the net receiving measures of WIN are at their lowest level while the opposite is true in the case of GEO.

5.3 Portfolio and risk management

In this section, we discuss and interpret the results with respect to bivariate and multivariate hedging and minimum-risk portfolios. We proceed by evaluating the performance of the multivariate portfolios using well-established measures such as hedging effectiveness (Ederington, 1979) and various Sharpe ratio metrics (Sharpe, 1994). Additionally, we conduct a comparative analysis of the constructed multivariate portfolios against the GRE, which serves as the current market portfolio, employing the information ratio as a key metric for assessment.

We begin by analyzing the performance of the individual series, examining key metrics such as annualized return, annualized standard deviation, and three different Sharpe ratios based on various risk measures. These findings are presented in Table 6.

We start by looking at the performance of the individual series. Table 6 shows the annualized return, annualized standard deviation as well as three Sharpe ratios that are based on different risk measures. As we can see SOL has the highest annual return of 13% followed by WIN with 10.1%, GRE with 8.5%, and GEO with 3.4%. Nevertheless, we should also take into consideration the annualized risk that comes with each asset. The lowest risk can be obtained by investing in GRE which serves as a market portfolio (18.2%), followed by GEO (26.8%), WIN (27.2%), and SOL (33.3%). Notably, we see a direct relationship: The higher the returns, the higher the risk.

[INSERT TABLE 6 AROUND HERE.]

Upon examining the original Sharpe ratio, which represents the return per standard deviation, it becomes evident that GRE emerges as the most appealing investment with the highest value (0.470). It is closely followed by SOL (0.391), WIN (0.373), and GEO (0.127). Similarly, when considering the Sharpe ratio based on VaR at the 5% quantile level, a similar ranking emerges, with SOL being the most attractive investment (2.371), followed by WIN (2.339), GRE (2.324), and GEO (1.789). In terms of the Sharpe ratio based on the CVaR at the 5% quantile level, SOL stands out as the most attractive option (2.371), followed closely by WIN (2.339), GRE (2.324), and GEO (1.789).

5.3.1 Hedging portfolios

When it comes to hedging portfolios, the primary objective is to minimize both risk and return by effectively hedging one asset with another or multiple assets. Thus, theoretically, the optimal hedge should aim for returns and risk to be close to zero, along with the Sharpe ratio. This is caused by the fact that hedges are commonly employed to safeguard the worth of an investment or portfolio rather than to generate extra profits. By striving for a zero return, the hedge plays a role in maintaining the overall position's value relatively steady, irrespective of shifts in the market.

To achieve this, we employ the bivariate hedge ratio technique developed by Kroner and Sultan (1993) to hedge one asset with another. Table 7 presents the results of this technique, revealing a significant reduction in investment risk for all asset pairs. Notably, the largest decrease in variance, amounting to 53.6%, is achieved by hedging GRE with SOL. Similarly, hedging SOL with GRE results in the second largest reduction, lowering the initial investment risk by 46.8%.

The empirical results reveal a consistent decrease in both annualized returns and annualized standard deviations across all cases. This decline is also reflected in lower Sharpe ratios, except for the GRE/GEO pair, which exhibited a higher Sharpe ratio of 0.537 compared to the original ratio of 0.470. Notably, the GEO/WIN and WIN/GRE pairs emerged as the most effective hedging combinations, generating annualized returns of -0.002 and 0.010, respectively. Moreover, the GEO/WIN pair demonstrates the most stable hedge ratio (10.5%), with a mean of 0.255. Consequently, a 1 USD investment in GEO can be hedged by shorting WIN by 0.255 USD.

[INSERT TABLE 7 AROUND HERE.]

When evaluating our proposed multivariate hedging technique, as presented in Table 8, we observe that all hedging effectiveness metrics either improved or remained equal compared to their bivariate counterparts. Notably, the multivariate approach achieved a 60.5% reduction in investment risk for GRE and a 29.1% reduction for WIN, slightly higher than the bivariate hedge ratio reduction of 28.0%. Although the decrease is marginal, it is essential to consider that utilizing the multivariate hedging portfolio consistently yields superior performance in terms of percentage reduction in investment risk.

Furthermore, the empirical evidence indicates that the annualized returns and annualized standard deviations of the multivariate hedging portfolio are either lower or equal to those of the bivariate hedge ratios, with the exception of the annualized returns for WIN/GRE and GEO. This trend is also observed in the Sharpe Ratios.

Additionally, it is worth mentioning that the incorporation of additional hedging factors could have potentially introduced noise and adversely affected the performance of the multivariate hedging portfolio. In summary, the multivariate hedging portfolio demonstrates a notable advantage over its bivariate counterpart in terms of risk mitigation for investments by lowering annualized returns and decreasing standard deviations, leading to generally lower Sharpe ratios in most instances.

[INSERT TABLE 8 AROUND HERE.]

5.3.2 Minimum risk portfolios

We will now explore bivariate and multivariate portfolio techniques aimed at minimizing risk while indirectly maximizing the Sharpe ratio, which reflects the highest return attainable given a specific level of investment risk. Our analysis begins with the empirical findings of Kroner and Ng (1998), who provide optimal bivariate portfolio weights in Table 9. The results indicate that not all bivariate portfolios result in a significant reduction in investment risk. For instance, when constructing a portfolio between GRE and SOL, we observe a slight increase of 1.5% in investment risk compared to GRE alone. Similarly, portfolios involving GRE and WIN or GEO show minor reductions in risk, which are only statistically significant at the 10% and 5% significance levels, respectively. Interestingly, the portfolio comprising GRE and SOL demonstrates a slight improvement in the Sharpe ratio, increasing from 0.470 to 0.481. However, this limited risk reduction in the portfolio can be attributed to the substantial weight assigned to GRE, which ranges between 0.971 and 1.000 in 95% of cases. Moreover, our analysis reveals that all combinations involving GRE yield high Sharpe ratios, while bivariate portfolios involving alternative energy sources reach a maximum Sharpe ratio of 0.393, significantly lower than 0.481. Consequently, a multivariate portfolio approach should be pursued to determine whether considering multiple assets can further enhance the Sharpe

ratio.

[INSERT TABLE 9 AROUND HERE.]

When considering multivariate portfolio techniques, one significant advantage is the ability to combine a variety of assets, which can potentially result in greater portfolio diversification and reduced investment risk. In this study, we compare several benchmark models: the minimum variance portfolio (Markowitz, 1952), the minimum correlation portfolio (Christoffersen et al., 2014), and the minimum connectedness portfolio (Broadstock et al., 2022). Additionally, we propose two portfolio frameworks: the minimum bivariate R^2 and the minimum R^2 decomposed connectedness portfolio.

Table 10 presents the empirical results of our multivariate portfolio analysis. Notably, the main distinction of the minimum variance portfolio by Markowitz (1952) is its focus on the GRE, with an average weight of 72.6%. Although this weight varies between 20.8% and 99.8%, investing predominantly in the GRE reduces the overall investment risk by 13.2%. Another significant finding is that alternative energy sources have small average weights, ranging from 1.7% to 18.1%. This observation aligns with the strategy employed by many investment companies, aiming to outperform a specific stock market index by investing a majority of their portfolio in the index and allocating the remainder to hand-selected stocks.

In contrast, the minimum correlation portfolio of Christoffersen et al. (2014) primarily focuses on alternative energy sources, with an average GRE weight of only 8.1%. The largest proportions are invested in GEO (34.6%), followed by WIN (31.1%), and SOL (26.2%). Table 3 and Figure 3 clearly demonstrate that GEO exhibits the lowest correlations with individual series, closely followed by WIN, SOL, and GRE. This strategy yields a Sharpe ratio of 0.508. It is important to note that this technique significantly reduces investment risk associated with alternative energy investments while substantially increasing the risk of investing solely in GRE. However, the Sharpe ratio, which represents returns relative to a given level of risk, is considerably higher for the minimum correlation portfolio compared to the minimum variance portfolio.

Next, we examine the minimum connectedness portfolio of Broadstock et al. (2022), which focuses on minimizing dynamic pairwise connectedness and interconnectedness

across series. While Tiwari et al. (2022) point out that the minimum correlation portfolio and the minimum connectedness portfolio lead to similar results, they have also found that the latter outperforms the former. This is also what we find in our empirical findings. It seems that the minimum connectedness portfolio attempts to combine elements of both the minimum variance and minimum correlation portfolios, as its weights fall within the bounds of these two benchmark frameworks. Notably, this approach outperforms both benchmarks as it reaches an annualized Sharpe ratio of 0.515.

[INSERT TABLE 10 AROUND HERE.]

Then, we focus on the minimum bivariate R^2 portfolio which can also be considered as a portfolio derived from the connectedness literature. In this event, we use the finding of Gabauer et al. (2023) that the (unscaled) GFEVD is equal to the bivariate R^2 goodness-of-fit measures. Thus, this approach is similar to the minimum correlation portfolio as it represents the squared dynamic conditional correlation measures while being derived from the connectedness approach of Diebold and Yılmaz (2012). Interestingly, we observe that the portfolio weights obtained using this technique are quite similar to those of the minimum correlation portfolio. However, the minimum correlation portfolio exhibits a slightly stronger representation for smaller weights and dampens the magnitude of larger weights. As a result, this technique leads to slightly higher hedging effectiveness metrics compared to the minimum correlation portfolio and also achieves a higher Sharpe ratio.

Finally, we shed light on the minimum R^2 decomposed connectedness portfolio. In contrast to the minimum connectedness portfolio and the minimum bivariate R^2 portfolio, this technique utilizes asymmetric connectedness measures, which provide additional insights into the predictive performance of the employed series. Since the diagonal elements are always equal to unity and each row sum is than unity, it can be assumed that the matrix is positive semidefinite and invertible. Although this portfolio technique yielded the lowest Sharpe ratio of 0.509 among the connectedness portfolios, it still outperforms both benchmarks. Moreover, the minimum R^2 decomposed connectedness portfolio not only exhibits significant superiority over the minimum variance portfolio in

terms of the Sharpe ratio but also enhances the hedging effectiveness of the minimum correlation portfolio.

5.3.3 Portfolio performance

In order to compare the various constructed portfolios with each other and with the current market portfolio, which is represented by the GRE, we conducted various statistical analyses. Table 11 reports a wide range of adjusted Sharpe ratios and the Information ratio between the GRE and various alternative portfolio techniques. Our empirical analysis reveals compelling evidence that the minimum bivariate R^2 portfolio consistently outperforms all other approaches. This conclusion is supported by the annualized Sharpe ratio, calculated based on standard deviation, Value-at-Risk, and Conditional Value-at-Risk, which consistently surpasses the alternatives. Similarly, the minimum connectedness portfolio developed by Broadstock et al. (2022) demonstrates superior performance, while the minimum R^2 decomposed connectedness portfolio presents striking results compared to the minimum correlation portfolio.

[INSERT TABLE 11 AROUND HERE.]

It is noteworthy that not only does the minimum correlation portfolio fall short, but all the connectedness-based portfolios consistently outperform the GRE, which serves as the market portfolio. Thus, we argue that constructing a portfolio based on the minimization of interconnectedness not only enhances the financial stability of the clean energy market but also yields a more stable market portfolio.

In conclusion, all three connectedness portfolios outperform both benchmarks while offering distinct methods for constructing portfolios. Introducing two additional connectedness portfolio techniques not only contributes to the risk and portfolio literature but also provides practical applications for measuring asset interconnectedness. Up until now, the connectedness literature has primarily focused on monitoring, predicting, and evaluating market risk. However, the work by Broadstock et al. (2022) stands out as the only one that offers a practical tool for estimating connectedness measures with direct relevance to risk and portfolio management.

6 Concluding remarks

In this study, we examine the return transmission mechanism among four clean energy indices: the NASDAQ OMX Green Economy Index (GRE), NASDAQ OMX Solar Energy Index (SOL), NASDAQ OMX Wind Energy Index (WIN), and NASDAQ OMX Geothermal Energy Index (GEO). Our analysis covers the period from December 1st, 2010 to June 2nd, 2023.

For this purpose, we have introduced a novel and efficient DCC-GARCH-based R^2 decomposed connectedness approach that allows us to examine connectedness measures in a time-varying fashion. This novel framework has been used in order to investigate the propagation mechanism across four renewable energy indices, we propose the novel and efficient DCC-GARCH-based R^2 decomposed connectedness approach. This approach does not only allow us to analyze connectedness measures in a time-varying fashion, but it also comes with the concept of dynamic conditional R^2 goodness-of-fit measure, which provides information about the expected degree of predictability.

We also introduce the minimum bivariate R^2 portfolio and the minimum R^2 decomposed connectedness portfolio, which aim to minimize interdependencies across series. Moreover, our study utilizes the dynamic conditional beta framework to model a multivariate hedging portfolio. The portfolio performance is evaluated based upon the Sharpe ratio (Sharpe, 1994) and the hedging effectiveness (Ederington, 1979).

The empirical findings reveal that the dynamic total connectedness varies over time and is influenced by economic events. Specifically, we identify three peaks associated with the Arab Spring in 2012, the COVID-19 pandemic in 2020, and the Russo-Ukrainian war in 2022. Furthermore, our results indicate that GRE acts as the primary net transmitter of shocks, while the other three alternative energy sources are net receivers of shocks. We also find that connectedness portfolios outperform minimum variance and minimum correlation portfolios. Additionally, creating bivariate and multivariate portfolios solely based on clean energy assets can significantly reduce portfolio risk. In fact, the multivariate hedging portfolio reduces the risk of holding a single asset by at least 23%.

These empirical results offer several benefits for practitioners and policymakers.

The connectedness analysis reveals the propagation mechanism across renewable energy sources which is crucial for policymakers to understand cross-market interdependencies. Furthermore, the clean energy market spillover analysis is also essential to design effective investment strategies that have positive effects on the amount of funding from investors concerning green energy projects facilitating the path to net-zero economies.

While our study focuses exclusively on the interconnectedness of the clean energy market, avenues for future research could explore different financial assets and expand the network to include commodity markets such as agricultural, livestock, industrial, and precious metal markets.

References

Alkathery, M. A., Chaudhuri, K., and Nasir, M. A. (2022). Implications of clean energy, oil and emissions pricing for the GCC energy sector stock. *Energy Economics*, 112:106119.

Anscombe, F. J. and Glynn, W. J. (1983). Distribution of the kurtosis statistic B2 for normal samples. *Biometrika*, 70(1):227–234.

Antonakakis, N., Chatziantoniou, I., and Gabauer, D. (2020a). Refined measures of dynamic connectedness based on time-varying parameter vector autoregressions. *Journal of Risk and Financial Management*, 13(4):84.

Antonakakis, N., Chatziantoniou, I., and Gabauer, D. (2021). The impact of Euro through time: Exchange rate dynamics under different regimes. *International Journal of Finance and Economics*, 26(1):1375–1408.

Antonakakis, N., Cunado, J., Filis, G., Gabauer, D., and de Gracia, F. P. (2020b). Oil and asset classes implied volatilities: Investment strategies and hedging effectiveness. *Energy Economics*, 91:104762.

Antonakakis, N., Gabauer, D., and Chatziantoniou, I. (2023). What is driving connectedness? Stylized facts from mean and volatility dynamics. *Stylized Facts from Mean and Volatility Dynamics (April 2, 2023)*.

Asl, M. G., Canarella, G., and Miller, S. M. (2021). Dynamic asymmetric optimal portfolio allocation between energy stocks and energy commodities: Evidence from clean energy and oil and gas companies. *Resources Policy*, 71:101982.

Balcilar, M., Gabauer, D., and Umar, Z. (2021). Crude oil futures contracts and commodity markets: New evidence from a TVP-VAR extended joint connectedness approach. *Resources Policy*, 73:102219.

Balli, F., Balli, H. O., Dang, T. H. N., and Gabauer, D. (2023). Contemporaneous and lagged R2 decomposed connectedness approach: New evidence from the energy futures market. *Finance Research Letters*, page 104168.

Baruník, J. and Křehlík, T. (2018). Measuring the frequency dynamics of financial connectedness and systemic risk. *Journal of Financial Econometrics*, 16(2):271–296.

Bloomberg (2019). New energy outlook 2019. https://www.gihub.org/resources/publications/bnef-new-energy-outlook-2019/. Accessed: 2023-08-08.

Bohl, M. T., Kaufmann, P., and Stephan, P. M. (2013). From hero to zero: Evidence of performance reversal and speculative bubbles in German renewable energy stocks. *Energy Economics*, 37:40–51.

Bollerslev, T. (1986). Generalized autoregressive conditional heteroskedasticity. *Journal of Econometrics*, 31(3):307–327.

Bollerslev, T. (1990). Modelling the coherence in short-run nominal exchange rates: A multivariate generalized ARCH model. *The Review of Economics and Statistics*, pages 498–505.

Bouoiyour, J., Gauthier, M., and Bouri, E. (2023). Which is leading: Renewable or brown energy assets? *Energy Economics*, 117:106339.

Bouri, E., Cepni, O., Gabauer, D., and Gupta, R. (2021). Return connectedness across asset classes around the COVID-19 outbreak. *International Review of Financial Analysis*, 73:101646.

Broadstock, D. C., Chan, K., Cheng, L. T., and Wang, X. (2021). The role of ESG performance during times of financial crisis: Evidence from COVID-19 in China. *Finance Research Letters*, 38:101716.

Broadstock, D. C., Chatziantoniou, I., and Gabauer, D. (2022). Minimum connectedness portfolios and the market for green bonds: Advocating socially responsible investment (SRI) activity. In *Applications in Energy Finance*, pages 217–253. Springer.

Burke, M. J. and Stephens, J. C. (2018). Political power and renewable energy futures: A critical review. *Energy Research and Social Science*, 35:78–93.

Caloia, F. G., Cipollini, A., and Muzzioli, S. (2019). How do normalization schemes affect net spillovers? A replication of the Diebold and Yilmaz (2012) study. *Energy Economics*, 84:104536.

Chatziantoniou, I., Abakah, E. J. A., Gabauer, D., and Tiwari, A. K. (2022). Quantile time–frequency price connectedness between green bond, green equity, sustainable investments and clean energy markets. *Journal of Cleaner Production*, 361:132088.

Chatziantoniou, I. and Gabauer, D. (2021). EMU-risk synchronisation and financial fragility through the prism of dynamic connectedness. *Quarterly Review of Economics and Finance*.

Chatziantoniou, I., Gabauer, D., and Stenfors, A. (2021). Interest rate swaps and the transmission mechanism of monetary policy: A quantile connectedness approach. *Economics Letters*, 204:109891.

Christoffersen, P., Errunza, V., Jacobs, K., and Jin, X. (2014). Correlation dynamics and international diversification benefits. *International Journal of Forecasting*, 30(3):807–824.

Christoffersen, P., Hahn, J., and Inoue, A. (2001). Testing and comparing value-at-risk measures. *Journal of empirical finance*, 8(3):325–342.

Christoffersen, P. and Pelletier, D. (2004). Backtesting value-at-risk: A duration-based approach. *Journal of Financial Econometrics*, 2(1):84–108.

Christoffersen, P. F. (1998). Evaluating interval forecasts. *International Economic Review*, pages 841–862.

D'Agostino, R. B. (1970). Transformation to normality of the null distribution of g1. *Biometrika*, pages 679–681.

Demiralay, S., Gencer, G., and Kilincarslan, E. (2023). Risk-return profile of environmentally friendly assets: Evidence from the NASDAQ OMX green economy index family. *Journal of Environmental Management*, 337:117683.

Diebold, F. X. and Yılmaz, K. (2009). Measuring financial asset return and volatility spillovers, with application to global equity markets. *Economic Journal*, 119(534):158–171.

Diebold, F. X. and Yılmaz, K. (2012). Better to give than to receive: Predictive directional measurement of volatility spillovers. *International Journal of Forecasting*, 28(1):57–66.

Diebold, F. X. and Yılmaz, K. (2014). On the network topology of variance decompositions: Measuring the connectedness of financial firms. *Journal of Econometrics*, 182(1):119–134.

Ding, Z., Granger, C. W., and Engle, R. F. (1993). A long memory property of stock market returns and a new model. *Journal of Empirical Finance*, 1(1):83–106.

Dogan, E., Madaleno, M., Taskin, D., and Tzeremes, P. (2022). Investigating the spillovers

and connectedness between green finance and renewable energy sources. *Renewable Energy*, 197:709–722.
Dutta, A. (2019). Impact of silver price uncertainty on solar energy firms. *Journal of Cleaner Production*, 225:1044–1051.
Ederington, L. H. (1979). The hedging performance of the new futures markets. *The Journal of Finance*, 34(1):157–170.
Elliott, G., Rothenberg, T. J., and Stock, J. H. (1996). Efficient tests for an autoregressive unit root. *Econometrica*, 64(4):813–836.
Engle, R. (2002). Dynamic conditional correlation: A simple class of multivariate generalized autoregressive conditional heteroskedasticity models. *Journal of Business and Economic Statistics*, 20(3):339–350.
Engle, R. and Sheppard, K. (2001). Theoretical and empirical properties of dynamic conditional correlation multivariate GARCH. Technical report, Department of Economics, UC San Diego.
Engle, R. F. (2016). Dynamic conditional beta. *Journal of Financial Econometrics*, 14(4):643–667.
Engle, R. F. and Bollerslev, T. (1986). Modelling the persistence of conditional variances. *Econometric Reviews*, 5(1):1–50.
Engle, R. F. and Ng, V. K. (1993). Measuring and testing the impact of news on volatility. *Journal of Finance*, 48(5):1749–1778.
Fisher, T. J. and Gallagher, C. M. (2012). New weighted Portmanteau statistics for time series goodness of fit testing. *Journal of the American Statistical Association*, 107(498):777–787.
Gabauer, D., Chatziantoniou, I., and Stenfors, A. (2023). Model-free connectedness measures. *Finance Research Letters*.
Genizi, A. (1993). Decomposition of R2 in multiple regression with correlated regressors. *Statistica Sinica*, pages 407–420.
Ghalanos, A. (2020). Introduction to the rugarch package. https://cran.r-project.org/web/packages/rugarch/vignettes/Introduction_to_the_rugarch_package.pdf. Accessed: 2023-11-27.
Glosten, L. R., Jagannathan, R., and Runkle, D. E. (1993). On the relation between the expected value and the volatility of the nominal excess return on stocks. *The Journal of Finance*, 48(5):1779–1801.
Gong, X.-L., Zhao, M., Wu, Z.-C., Jia, K.-W., and Xiong, X. (2023). Research on tail risk contagion in international energy markets - The quantile time-frequency volatility spillover perspective. *Energy Economics*, 121:106678.
Goodell, J. W., Corbet, S., Yadav, M. P., Kumar, S., Sharma, S., and Malik, K. (2022). Time and frequency connectedness of green equity indices: Uncovering a socially important link to Bitcoin. *International Review of Financial Analysis*, 84:102379.
Gustafsson, R., Dutta, A., and Bouri, E. (2022). Are energy metals hedges or safe havens for clean energy stock returns? *Energy*, 244:122708.
Ha, L. T. (2023). Dynamic connectedness between green energy and carbon risk during Russia-Ukraine conflict: new evidence from a wavelet analysis. *Environmental Science and Pollution Research*, pages 1–18.
Hanif, W., Mensi, W., Gubareva, M., and Teplova, T. (2023). Impacts of COVID-19 on dynamic return and volatility spillovers between rare earth metals and renewable energy stock markets. *Resources Policy*, 80:103196.
Hansen, P. R. and Lunde, A. (2005). A forecast comparison of volatility models: Does anything beat a GARCH (1, 1)? *Journal of Applied Econometrics*, 20(7):873–889.
Hentschel, L. (1995). All in the family nesting symmetric and asymmetric GARCH models. *Journal of Financial Economics*, 39(1):71–104.
Higgins, M. L., Bera, A. K., et al. (1992). A class of nonlinear ARCH models. *International*

Economic Review, 33(1):137–158.

International Energy Agency (2022). World energy outlook 2022. https://www.iea.org/reports/world-energy-outlook-2022. Accessed: 2023-11-27.

International Renewable Energy Agency (2021). Renewable capacity statistics 2021. https://www.irena.org/publications/2021/March/Renewable-Capacity-Statistics-2021. Accessed: 2023-11-27.

Jaeger, J. (2021). Explaining the exponential growth of renewable energy. https://www.wri.org/insights/growth-renewable-energy-sector-explained?trk=public_post_comment-text. Accessed: 2023-11-27.

Jarque, C. M. and Bera, A. K. (1980). Efficient tests for normality, homoscedasticity and serial independence of regression residuals. *Economics Letters*, 6(3):255–259.

Kirschbaum, E. (2011). Arab spring helps desertec's solar energy plan: Ceo. https://www.reuters.com/article/us-climate-desertec-idUSTRE7A26YA20111103. Accessed: 2023-08-08.

Koop, G., Pesaran, M. H., and Potter, S. M. (1996). Impulse response analysis in nonlinear multivariate models. *Journal of Econometrics*, 74(1):119–147.

Kroner, K. F. and Ng, V. K. (1998). Modeling asymmetric movements of asset prices. *Review of Financial Studies*, 11(04):817–844.

Kroner, K. F. and Sultan, J. (1993). Time-varying distributions and dynamic hedging with foreign currency futures. *Journal of Financial and Quantitative Analysis*, 28(04):535–551.

Kuang, W. (2021). Are clean energy assets a safe haven for international equity markets? *Journal of Cleaner Production*, 302:127006.

Lastrapes, W. D. and Wiesen, T. F. (2021). The joint spillover index. *Economic Modelling*, 94:681–691.

Lee, C.-C., Wang, F., and Chang, Y.-F. (2023). Does green finance promote renewable energy? Evidence from China. *Resources Policy*, 82:103439.

Li, J., Liang, H., and Ni, L. (2023a). Quantile VAR network evidence for spillover effects and connectivity between China's stock markets, green commodities, and Bitcoin. *Environmental Science and Pollution Research*, pages 1–19.

Li, J., Umar, M., and Huo, J. (2023b). The spillover effect between Chinese crude oil futures market and Chinese green energy stock market. *Energy Economics*, 119:106568.

Li, K., Bian, H., Liu, C., Zhang, D., and Yang, Y. (2015). Comparison of geothermal with solar and wind power generation systems. *Renewable and Sustainable Energy Reviews*, 42:1464–1474.

Liu, N., Liu, C., Da, B., Zhang, T., and Guan, F. (2021). Dependence and risk spillovers between green bonds and clean energy markets. *Journal of Cleaner Production*, 279:123595.

Lv, C., Fan, J., and Lee, C.-C. (2023). Can green credit policies improve corporate green production efficiency? *Journal of Cleaner Production*, 397:136573.

Markowitz, H. (1952). Selection portfolio. *The Journal of Finance*, 7(1):77–91.

Mensi, W., Shafiullah, M., Vo, X. V., and Kang, S. H. (2022). Spillovers and connectedness between green bond and stock markets in bearish and bullish market scenarios. *Finance Research Letters*, 49:103120.

Naeem, M. A., Chatziantoniou, I., Gabauer, D., and Karim, S. (2023). Measuring the G20 stock market return transmission mechanism: Evidence from the R2 connectedness approach. *International Review of Financial Analysis*.

Naeem, M. A., Karim, S., Farid, S., and Tiwari, A. K. (2022). Comparing the asymmetric efficiency of dirty and clean energy markets pre and during COVID-19. *Economic Analysis and Policy*, 75:548–562.

Nelson, D. B. (1991). Conditional heteroskedasticity in asset returns: A new approach. *Econometrica*, 59(2):347–370.

Patel, R., Kumar, S., Bouri, E., and Iqbal, N. (2023). Spillovers between green and

dirty cryptocurrencies and socially responsible investments around the war in Ukraine. *International Review of Economics and Finance*, 87:143–162.

Pesaran, H. H. and Shin, Y. (1998). Generalized impulse response analysis in linear multivariate models. *Economics Letters*, 58(1):17–29.

Ren, B. and Lucey, B. (2022). A clean, green haven? - Examining the relationship between clean energy, clean and dirty cryptocurrencies. *Energy Economics*, 109:105951.

Schwert, G. W. (1990). Stock volatility and the crash of '87. *Review of Financial Studies*, 3(1):77–102.

Sharpe, W. F. (1994). The Sharpe ratio. *Journal of Portfolio Management*, 21(1):49–58.

Tiwari, A. K., Abakah, E. J. A., Gabauer, D., and Dwumfour, R. A. (2022). Dynamic spillover effects among green bond, renewable energy stocks and carbon markets during COVID-19 pandemic: Implications for hedging and investments strategies. *Global Finance Journal*, 51:100692.

Umar, M., Riaz, Y., and Yousaf, I. (2022). Impact of Russian-Ukraine war on clean energy, conventional energy, and metal markets: Evidence from event study approach. *Resources Policy*, 79:102966.

Yahya, F., Abbas, G., and Lee, C.-C. (2023). Asymmetric effects and volatility transmission from metals markets to solar energy stocks: Evidence from DCC, ADCC, and quantile regression approach. *Resources Policy*, 82:103501.

Zakoian, J.-M. (1994). Threshold heteroskedastic models. *Journal of Economic Dynamics and Control*, 18(5):931–955.

Zeng, H., Lu, R., and Ahmed, A. D. (2023). Return connectedness and multiscale spillovers across clean energy indices and grain commodity markets around COVID-19 crisis. *Journal of Environmental Management*, 340:117912.

Zeqiraj, V., Sohag, K., and Soytas, U. (2020). Stock market development and low-carbon economy: The role of innovation and renewable energy. *Energy Economics*, 91:104908.

Zhang, D., Chen, X. H., Lau, C. K. M., and Cai, Y. (2023). The causal relationship between green finance and geopolitical risk: Implications for environmental management. *Journal of Environmental Management*, 327:116949.

Table 1: Summary statistics

	GRE	SOL	WIN	GEO
Mean	0.039*	0.071*	0.053*	0.027
	(0.055)	(0.059)	(0.082)	(0.362)
Variance	1.311***	4.390***	2.934***	2.852***
Skewness	-0.517***	-0.175***	-0.137***	0.718***
	(0.000)	(0.000)	(0.002)	(0.000)
Ex.Kurtosis	9.089***	4.599***	3.734***	14.437***
	(0.000)	(0.000)	(0.000)	(0.000)
JB	10990.261***	2794.169***	1840.851***	27644.162***
	(0.000)	(0.000)	(0.000)	(0.000)
ERS	-6.053***	-9.569***	-11.933***	-11.570***
	(0.000)	(0.000)	(0.000)	(0.000)
$Q^2(20)$	2312.705***	1585.716***	247.003***	324.849***
	(0.000)	(0.000)	(0.000)	(0.000)
	Kendall rank correlation coefficients			
GRE	1.000***	0.483***	0.360***	0.309***
SOL	0.483***	1.000***	0.269***	0.242***
WIN	0.360***	0.269***	1.000***	0.185***
GEO	0.309***	0.242***	0.185***	1.000***

Notes: ***,**,* denote significance at 1%, 5%, and 10% significance levels while values in parentheses represent p-values; Skewness: D'Agostino (1970) test; Kurtosis: Anscombe and Glynn (1983) test; JB: Jarque and Bera (1980) normality test; ERS: Elliott et al. (1996) unit-root test; $Q^2(20)$: Fisher and Gallagher (2012) weighted Portmanteau test statistics.

Table 2: Connectedness table schematic

	x_1	x_2	$\cdots$	x_K	$FROM_t$
x_1	1	$R^{2d}_{12,t}$	$\cdots$	$R^{2d}_{1K,t}$	$\sum_{j=1,j\neq 1}^{K} R^{2d}_{1j,t} = R^2_{1,t}$
x_2	$R^{2d}_{21,t}$	1	$\cdots$	$R^{2d}_{2K,t}$	$\sum_{j=1,j\neq 2}^{K} R^{2d}_{2j,t} = R^2_{2,t}$
$\vdots$	$\vdots$	$\vdots$	$\ddots$	$\vdots$	$\vdots$
x_K	$R^{2d}_{K1,t}$	$R^{2d}_{K2,t}$	$\cdots$	1	$\sum_{j=1,j\neq K}^{K} R^{2d}_{Kj,t} = R^2_{K,t}$
TO_t	$\sum_{j=1,j\neq 1}^{K} R^{2d}_{j1,t}$	$\sum_{j=1,j\neq 2}^{K} R^{2d}_{j2,t}$	$\cdots$	$\sum_{j=1,j\neq K}^{K} R^{2d}_{jK,t}$	TCI_t
NET_t	$TO_{1,t} - FROM_{1,t}$	$TO_{2,t} - FROM_{2,t}$	$\cdots$	$TO_{K,t} - FROM_{K,t}$	$\frac{1}{K}\sum_{k=1}^{K} R^2_{i,t}$

Table 3: Bivariate DCC-GARCH(1,1) with mixed univariate GARCH estimation table

	GRE	SOL	WIN	GEO
	Univariate GARCH parameters			
	Exponential GARCH	Bollerslev GARCH	Threshold GARCH	Threshold GARCH
μ	0.042***	0.070***	0.070***	0.011
ω	-0.004	0.057	0.039	0.026
α	0.177***	0.057***	0.075**	0.085*
β	0.984***	0.929***	0.920***	0.922***
γ	-0.106***		0.386***	0.323***
	Conditional distribution parameters			
	SSTD	SGED	STD	SSTD
shape	7.414***	1.346***	5.424***	4.173***
skew	0.873***	0.978***		0.918***
	Multivariate GARCH parameters: a \ b			
GRE		0.937***	0.988***	0.937***
SOL	0.042***		0.986***	0.963***
WIN	0.009***	0.012***		0.985***
GEO	0.034***	0.025***	0.010***	
	DCC \ Student's t dof			
GRE		10.169***	9.304***	8.217***
SOL	0.649***		11.057***	10.888***
WIN	0.514***	0.396***		9.511***
GEO	0.421***	0.339***	0.275***	

Notes: Estimation results of DCC-GARCH (Engle, 2002) with mixed univariate GARCH models (Antonakakis et al., 2021); ***,**,* denote significance at 1%, 5%, and 10% significance levels while values in parentheses represent p-values. STD: Student's t; SSTD: skew Student's t; SGED: skew generalized error distribution,

Table 4: Evaluation of univariate GARCH performance

	Sign Bias	$Q^2(20)$	VaR	CVaR	VaR Dur.
GRE	1.111	12.775	1.955	−678.032	1.115
	(0.267)	(0.248)	(0.162)	(0.943)	(0.770)
SOL	1.618	15.327	2.673	−686.697	1.134
	(0.106)	(0.108)	(0.102)	(0.933)	(0.933)
WIN	0.753	4.927	2.422	−683.814	1.127
	(0.451)	(0.959)	(0.120)	(0.870)	(0.540)
GEO	0.510	6.609	0.001	−627.929	1.006
	(0.610)	(0.857)	(0.974)	(0.700)	(0.583)

Notes: Notes: ***,**,* denote significance at 1%, 5%, and 10% significance levels while values in parentheses represent p-values. Sign Bias: Engle and Ng (1993) test; $Q^2(20)$: Weighted Portmanteau test statistics (Fisher and Gallagher, 2012); VaR: Value-at-Risk test (Christoffersen, 1998); CVaR: Conditional Value-at-Risk test (Christoffersen et al., 2001); VaR Dur.: Value-at-Risk Duration (Christoffersen and Pelletier, 2004). All VaR test statistics are based on the 5% quantile level.

Table 5: Averaged connectedness measures

	GRE	SOL	WIN	GEO	FROM
GRE	100.00	29.53	15.47	9.93	54.93
SOL	31.42	100.00	8.71	6.30	46.42
WIN	17.38	8.95	100.00	3.58	29.92
GEO	11.25	6.58	3.62	100.00	21.45
TO	60.05	45.06	27.79	19.81	152.72
Inc.Own	160.05	145.06	127.79	119.81	TCI
NET	5.12	-1.36	-2.13	-1.63	38.18

Notes: Averaged R^2 decomposed connectedness measures are based on a DCC-GARCH (Engle, 2002) with mixed univariate GARCH models (Antonakakis et al., 2021).

Table 6: Asset performance

	GRE	SOL	WIN	GEO
Return	0.085	0.130	0.101	0.034
Std.Dev.	0.182	0.333	0.272	0.268
Sharpe Ratio				
Std.Dev.	0.470	0.391	0.373	0.127
VaR	4.758	3.962	3.757	1.789
CVaR	2.324	2.371	2.339	1.789

Table 7: Hedge ratios

	Mean	Std.Dev.	5%	95%	HE	p-value	Return	Risk	SR
GRE/SOL	0.336	0.146	0.144	0.612	0.536	0.000	0.057	0.124	0.460
GRE/WIN	0.308	0.114	0.165	0.533	0.345	0.004	0.058	0.147	0.391
GRE/GEO	0.290	0.149	0.108	0.593	0.278	0.000	0.083	0.154	0.537
SOL/GRE	1.400	0.440	0.734	2.194	0.468	0.000	-0.015	0.243	-0.064
SOL/WIN	0.472	0.174	0.224	0.824	0.195	0.004	0.063	0.298	0.210
SOL/GEO	0.459	0.212	0.170	0.841	0.169	0.000	0.117	0.303	0.386
WIN/GRE	0.950	0.338	0.477	1.614	0.280	0.000	0.010	0.231	0.044
WIN/SOL	0.352	0.163	0.127	0.645	0.205	0.000	0.070	0.242	0.290
WIN/GEO	0.325	0.149	0.150	0.624	0.098	0.000	0.089	0.258	0.344
GEO/GRE	0.696	0.300	0.274	1.207	0.227	0.000	-0.045	0.236	-0.190
GEO/SOL	0.264	0.124	0.087	0.497	0.176	0.000	-0.021	0.243	-0.087
GEO/WIN	0.255	0.105	0.126	0.457	0.098	0.004	-0.002	0.255	-0.007

Notes: Results are based on the hedge ratio of Kroner and Sultan (1993), hedging effectiveness of Ederington (1979), and the test statistics for the hedging effectiveness of Antonakakis et al. (2020b).

Table 8: Multivariate hedging portfolios

	Mean	Std.Dev.	5%	95%	HE	p-value	Return	Risk	SR
GRE/SOL	0.251	0.123	0.086	0.490					
GRE/WIN	0.158	0.054	0.086	0.264	0.605	0.000	0.042	0.114	0.364
GRE/GEO	0.122	0.074	0.021	0.257					
SOL/GRE	1.234	0.492	0.571	2.154					
SOL/WIN	0.090	0.170	-0.173	0.353	0.474	0.000	-0.013	0.241	-0.055
SOL/GEO	0.088	0.136	-0.126	0.317					
WIN/GRE	0.804	0.351	0.304	1.383					
WIN/SOL	0.094	0.168	-0.168	0.397	0.291	0.000	0.025	0.229	0.107
WIN/GEO	0.064	0.076	-0.049	0.208					
GEO/GRE	0.521	0.288	0.119	1.003					
GEO/SOL	0.083	0.119	-0.101	0.289	0.228	0.000	-0.050	0.236	-0.214
GEO/WIN	0.059	0.074	-0.046	0.184					

Notes: Results are based on our proposed multivariate hedging strategy, hedging effectiveness of Ederington (1979), and the test statistics for the hedging effectiveness of Antonakakis et al. (2020b).

Table 9: Optimal bivariate portfolio weights

	Mean	Std.Dev.	5%	95%	HE	p-value	SR
GRE/SOL	0.971	0.096	0.791	1.000	-0.015	0.669	0.481
GRE/WIN	0.885	0.159	0.527	1.000	0.061	0.075	0.424
GRE/GEO	0.787	0.204	0.346	1.000	0.072	0.035	0.423
SOL/GRE	0.029	0.096	0.000	0.209	0.697	0.000	0.481
SOL/WIN	0.378	0.180	0.121	0.707	0.447	0.000	0.393
SOL/GEO	0.307	0.159	0.067	0.608	0.467	0.000	0.308
WIN/GRE	0.115	0.159	0.000	0.473	0.581	0.000	0.424
WIN/SOL	0.622	0.180	0.293	0.879	0.173	0.000	0.393
WIN/GEO	0.426	0.188	0.134	0.773	0.406	0.000	0.348
GEO/GRE	0.213	0.204	0.000	0.654	0.573	0.000	0.423
GEO/SOL	0.693	0.159	0.392	0.933	0.180	0.000	0.308
GEO/WIN	0.574	0.188	0.227	0.866	0.389	0.000	0.348

Notes: Results are based on the optimal bivariate portfolio weight framework of Kroner and Ng (1998), hedging effectiveness of Ederington (1979), and the test statistics for the hedging effectiveness of Antonakakis et al. (2020b).

Table 10: Multivariate portfolio analysis

	Mean	Std.Dev.	5%	95%	HE	p-value	SR
Minimum variance portfolio (MVP)							
GRE	0.726	0.247	0.208	0.998	0.132	0.000	0.404
SOL	0.017	0.061	0.000	0.131	0.741	0.000	
WIN	0.077	0.112	0.000	0.307	0.612	0.000	
GEO	0.181	0.165	0.000	0.542	0.601	0.000	
Minimum correlation portfolio (MCP)							
GRE	0.081	0.069	0.000	0.209	-0.345	0.000	0.508
SOL	0.262	0.065	0.129	0.345	0.598	0.000	
WIN	0.311	0.050	0.221	0.381	0.399	0.000	
GEO	0.346	0.032	0.286	0.391	0.382	0.000	
Minimum connectedness portfolio (MPP)							
GRE	0.136	0.053	0.042	0.220	-0.301	0.000	0.515
SOL	0.251	0.036	0.183	0.305	0.611	0.000	
WIN	0.294	0.031	0.240	0.341	0.419	0.000	
GEO	0.319	0.019	0.282	0.342	0.402	0.000	
Minimum bivariate R^2 portfolio (MRP)							
GRE	0.085	0.069	0.000	0.211	-0.343	0.000	0.527
SOL	0.259	0.066	0.128	0.342	0.599	0.000	
WIN	0.311	0.047	0.235	0.380	0.400	0.000	
GEO	0.344	0.032	0.287	0.397	0.383	0.000	
Minimum R^2 decomposed connectedness portfolio (M2P)							
GRE	0.200	0.017	0.173	0.231	-0.250	0.000	0.509
SOL	0.236	0.016	0.210	0.262	0.627	0.000	
WIN	0.273	0.018	0.241	0.301	0.442	0.000	
GEO	0.292	0.014	0.266	0.310	0.425	0.000	

Notes: Results are based on global minimum risk frameworks (Markowitz, 1952; Christoffersen et al., 2014; Broadstock et al., 2022), hedging effectiveness of Ederington (1979), and the test statistics for the hedging effectiveness of Antonakakis et al. (2020b).

Table 11: Portfolio performance

	MVP	MCP	MPP	MRP	M2P
Std.Dev. based Sharpe ratio	0.404	0.508	0.515	0.527	0.509
VaR based Sharpe ratio	4.417	5.432	5.505	5.633	5.389
CVaR based Sharpe ratio	2.921	3.409	3.458	3.503	3.274
Information ratio (GRE)	−0.223	0.157	0.165	0.187	0.150

Figure 1: Dynamic conditional variance-covariances

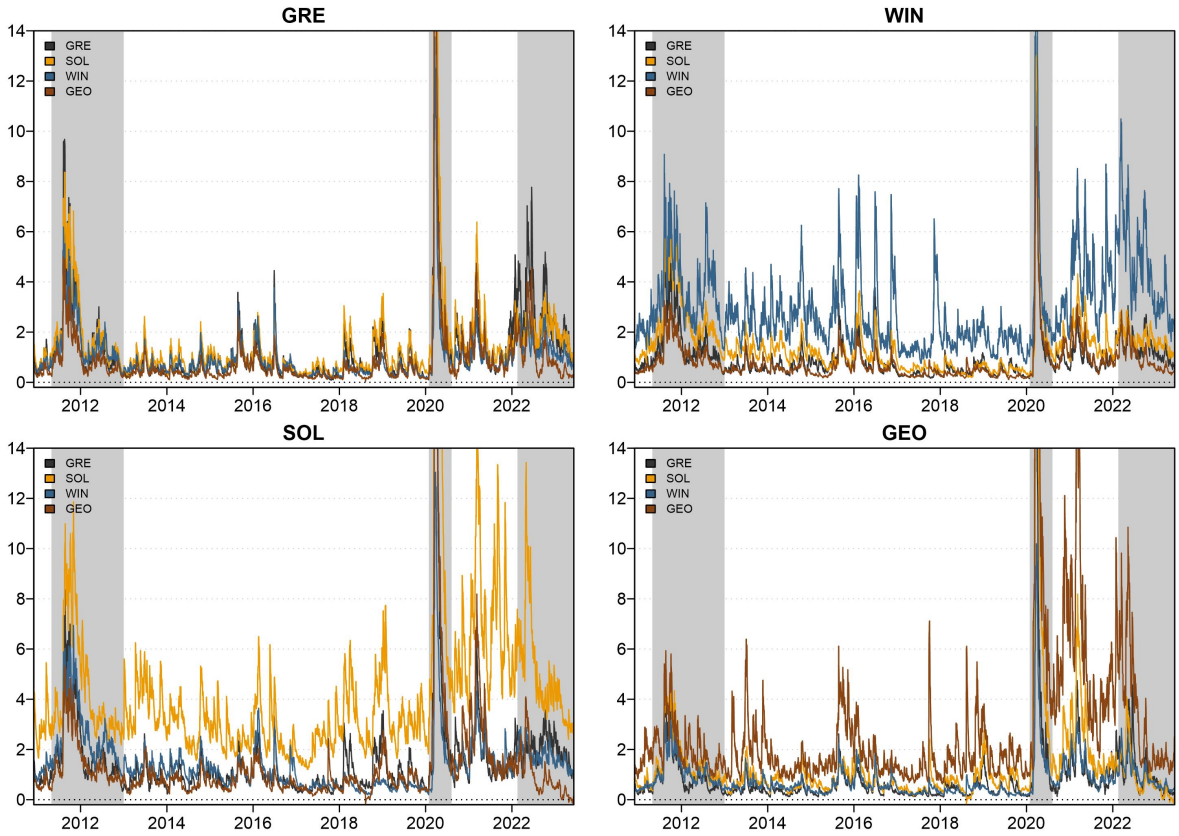

Notes: The dynamic conditional variances and covariances are retrieved from the DCC-GARCH framework (Engle, 2002) with mixed univariate GARCH models (Antonakakis et al., 2021).

Figure 2: Dynamic conditional betas

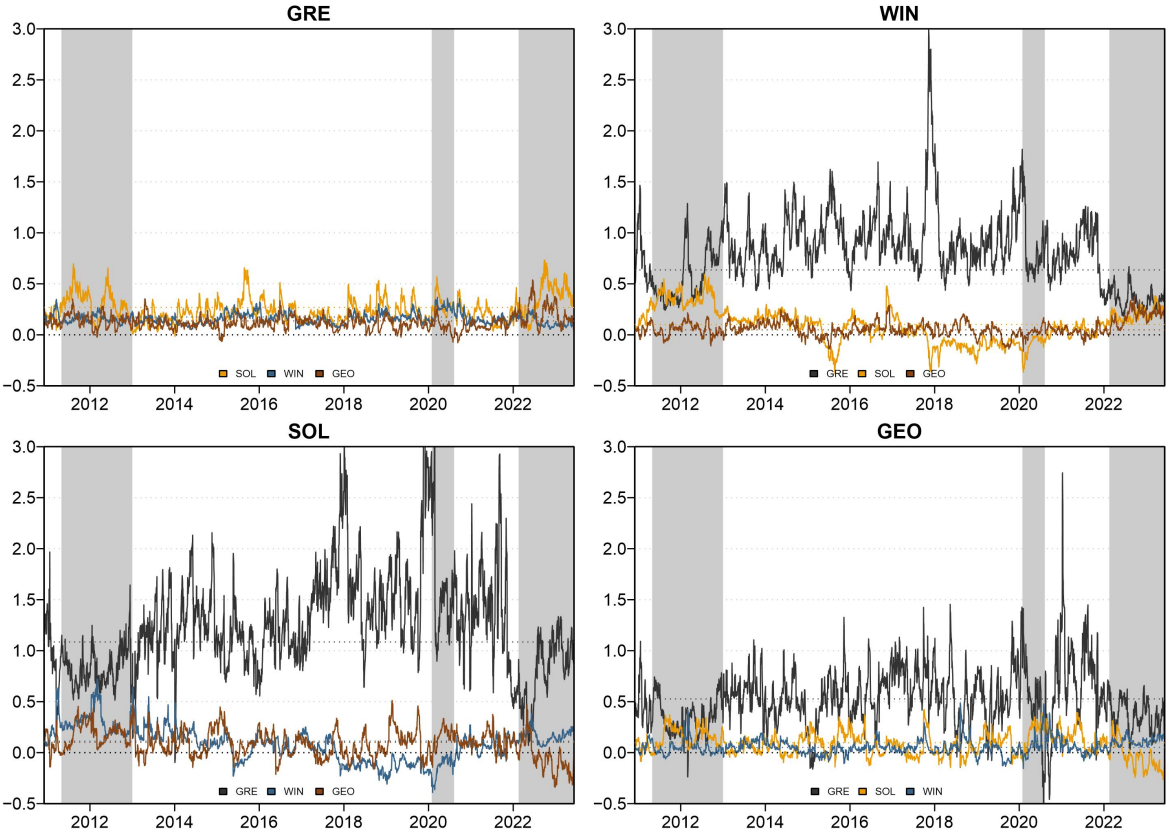

Notes: The dynamic conditional betas are retrieved from the DCC-GARCH framework (Engle, 2002) with mixed univariate GARCH models (Antonakakis et al., 2021).

Figure 3: Dynamic conditional correlations

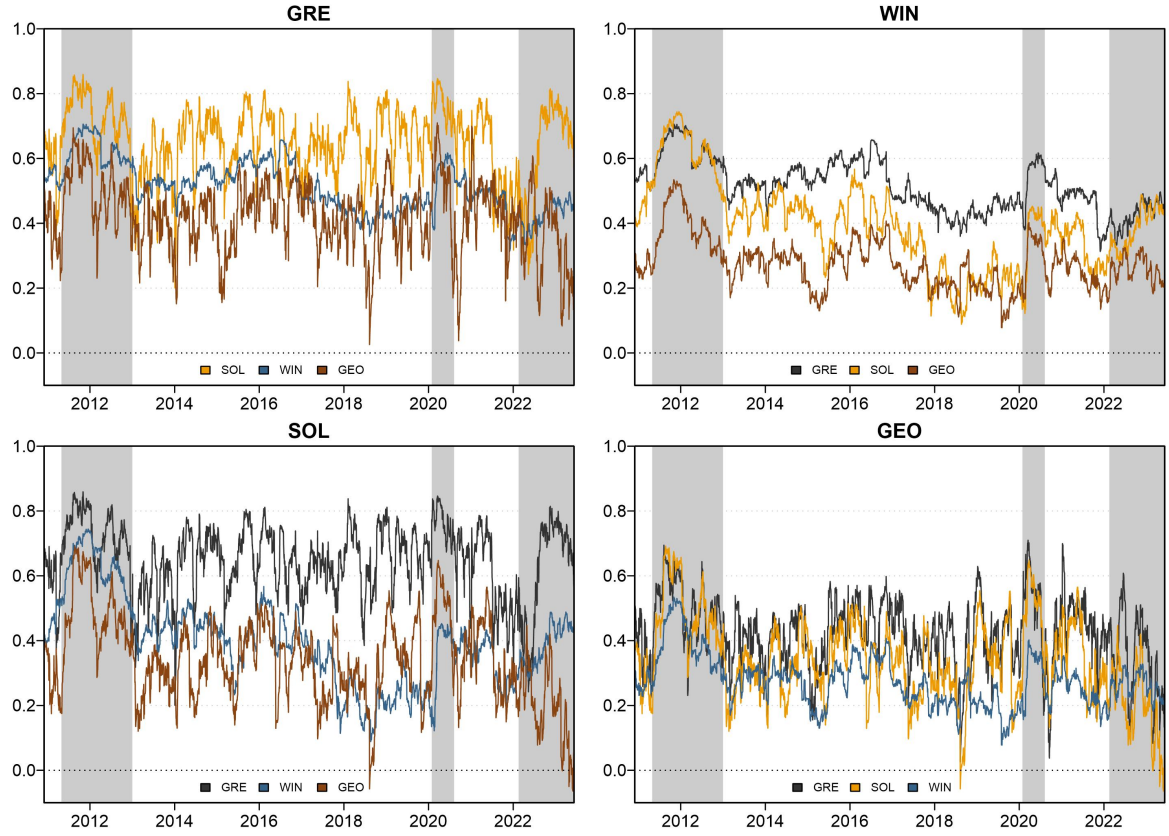

Notes: The dynamic conditional correlations are retrieved from the DCC-GARCH framework (Engle, 2002) with mixed univariate GARCH models (Antonakakis et al., 2021).

Figure 4: Dynamic conditional R^2 decomposed measures

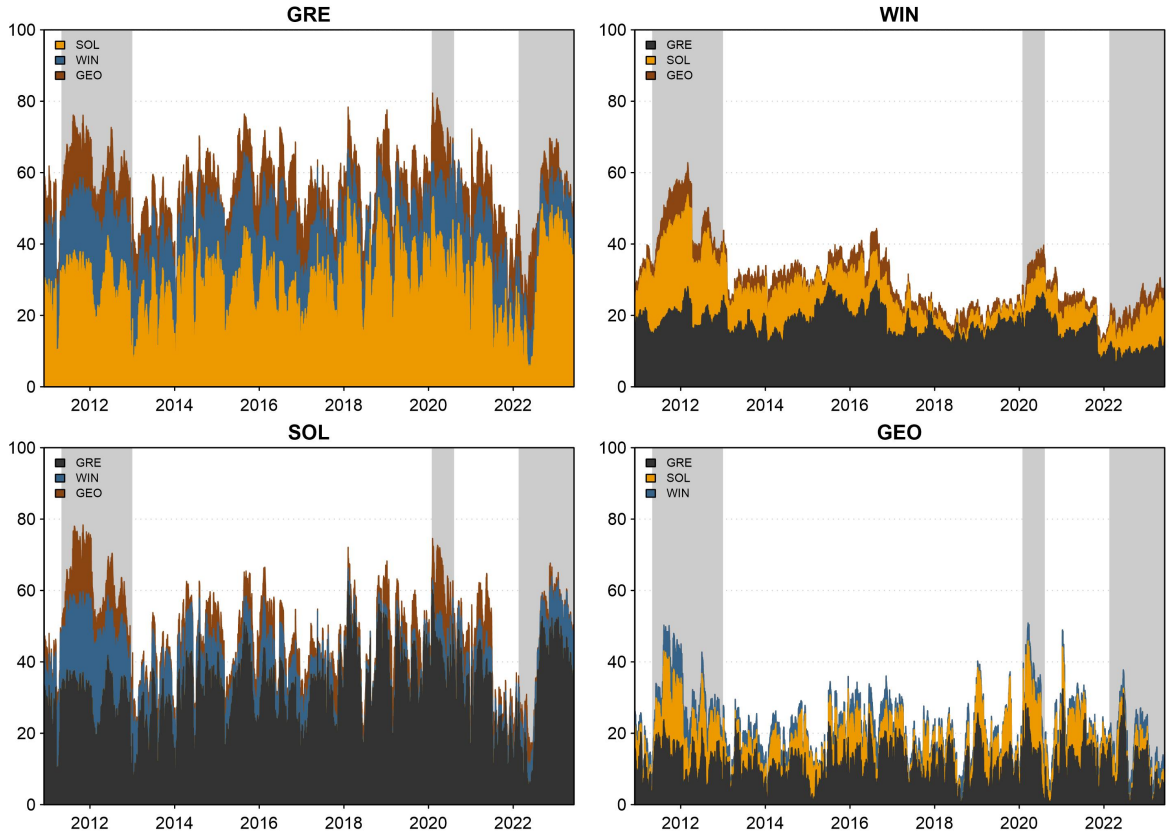

Notes: The dynamic conditional R^2 decomposed goodness-of-fit measures are based on the DCC-GARCH framework (Engle, 2002) with mixed univariate GARCH models (Antonakakis et al., 2021). and the R^2 decomposition approach of Genizi (1993).

Figure 5: Dynamic total connectedness

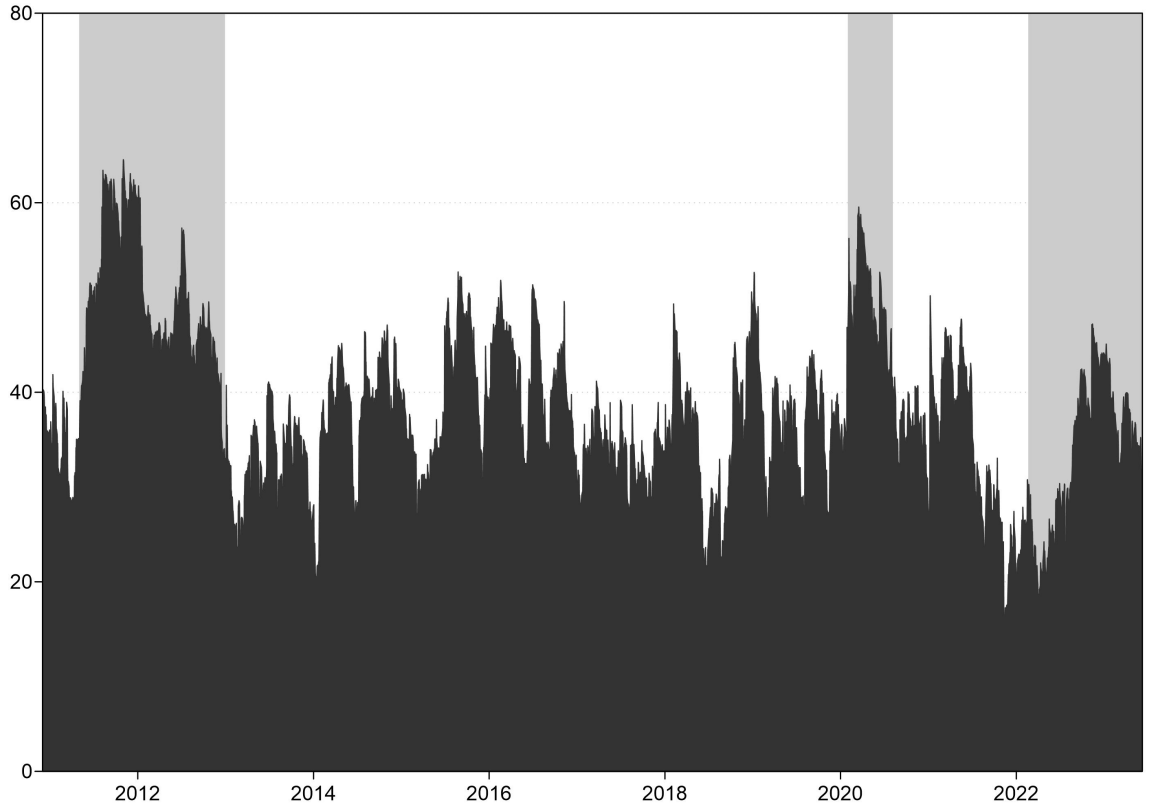

Notes: Dynamic total connectedness measures rest on the DCC-GARCH framework (Engle, 2002) with mixed univariate GARCH models (Antonakakis et al., 2021).

Figure 6: Net total directional connectedness

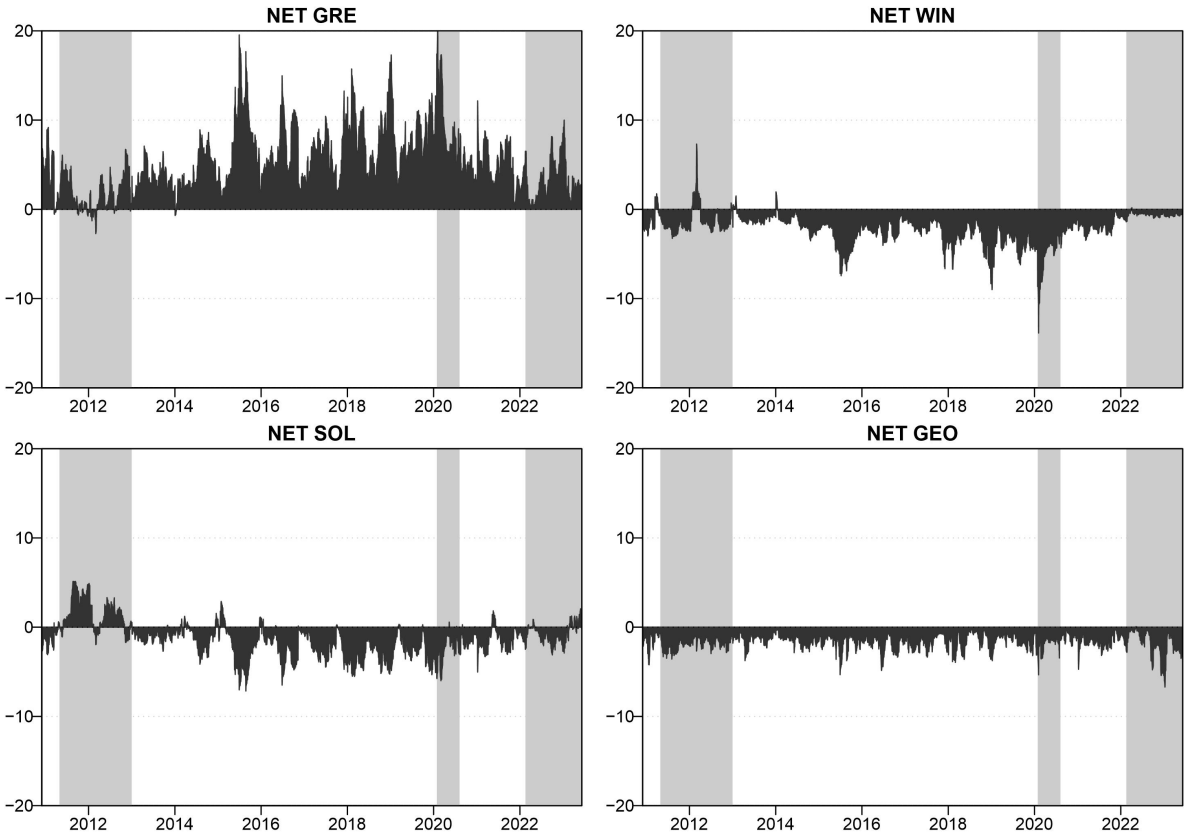

Notes: Net total directional connectedness measures rest on the DCC-GARCH framework (Engle, 2002) with mixed univariate GARCH models (Antonakakis et al., 2021).